FEATURE ARTICLE

Check for updates

Next-generation air filtration nanotechnology for improved indoor air quality

Hongchan Kim,[a] Junhyuk Oh,[a] Hakbeom Lee,[a] Seongmin Jeong*[a] and
Seung Hwan Ko [ID] *[abc]

Indoor air quality (IAQ) significantly affects human health, with pollutants such as organic, inorganic substances, and biological contaminants contributing to various respiratory, neurological, and immunological diseases. In this review, we highlighted the need for advanced air filtration technologies to mitigate these pollutants, which are emitted from household products, building materials, combustion processes, and bioaerosols. While traditional HVAC systems and mechanical filtration methods have been effective, they are often energy-intensive and limited in their ability to capture specific pollutants. To address these limitations, nanotechnology-based air filtration technologies, particularly those utilizing electrospinning processes, offer promising alternatives. This review classifies pollutants and details the working principles of next-generation filters, focusing on passive, self-powered, and externally powered mechanisms. These advanced filters achieve high filtration efficiency with minimal pressure drop, enhanced pollutant capture, and in some cases, health monitoring capabilities. This review emphasizes the significance of ongoing research into eco-friendly and sustainable filtration systems to enhance IAQ and minimize health risks linked to long-term exposure to indoor air pollutants.

1. Introduction

Air is essential for human survival. However, the importance of air quality has only recently begun to receive significant attention. Since industrialization and urbanization began in the 19th century, air pollution caused by anthropogenic activity has rapidly progressed.[1] It wasn't until the Great Smog of London in the 1950s, which resulted in the deaths of approximately 12 000 people, that the UK enacted the world's first legislation aimed at preventing air pollution in 1956.[2,3] In 1955,

[a] *Applied Nano and Thermal Science Lab, Department of Mechanical Engineering, Seoul National University, 1, Gwanak-ro, Gwanak-gu, Seoul, 08826, Republic of Korea. E-mail: jsm0817@snu.ac.kr, maxko@snu.ac.kr*

[b] *Institute of Engineering Research/Institute of Advanced Machinery and Design (SNU-IAMD), Seoul National University, 1, Gwanak-ro, Gwanak-gu, Seoul, 08826, Republic of Korea*

[c] *Interdisciplinary Program in Bioengineering, Seoul National University, 1, Gwanak-ro, Gwanak-gu, Seoul, 08826, Republic of Korea*

Hongchan Kim is a PhD student in the Applied Nano and Thermal Science Lab, led by Prof. Seung Hwan Ko's group at Seoul National University, South Korea. He received his BS in the Department of Mechanical Engineering from Konkuk University in 2022. His current research focuses on nanofiber electronics for energy-efficient air filtration.

Hongchan Kim

Junhyuk Oh is a PhD student in the Applied Nano and Thermal Science Lab, led by Prof. Seung Hwan Ko's group at Seoul National University, South Korea. He received his BS in the Department of Mechanical Engineering from Hongik University in 2024. His current research focuses on nanofiber electronics for energy-efficient air filtration and stretchable electrodes.

Junhyuk Oh

the United States also established regulations to control the emission of air pollutants.[4] Although air pollution reduction technologies and regulations have developed through these international discussions, and pollution levels have shown a decreasing trend,[5,6] humans are still surrounded by threats from numerous diseases, including respiratory illnesses, dermatitis, neurological disorders, and cardiovascular diseases, due to continuous exposure to air pollutants.[7–10]

Specifically, people today spend the majority of their time indoors, whether at home, in workplaces, or while commuting.[11,12] Indoor air pollution can be even more harmful to humans due to the confined space,[12] and as demonstrated by the recent COVID-19 pandemic, the transmission speed of infectious viruses in enclosed spaces is extremely fast.[13] As a result, recent studies have increasingly focused on the significance of indoor air quality (IAQ) for maintaining good health and comfort, accelerating research on IAQ improvement and monitoring.[14–16] Early research on IAQ improvement focused on ventilation technologies that effectively reduced indoor air pollution by mixing indoor and outdoor air through large heating, ventilation, & air conditioning (HVAC) systems.[17,18] However, such HVAC systems consume relatively large amounts of power and have limitations in

fundamentally capturing pollution sources, making it possible for them to generate pollutants on their own.[19] Therefore, more compact filtration technologies capable of directly capturing pollutants at the source have gained attention.[20]

The mechanisms of traditional filters are divided into mechanical and electrical filtration. Mechanical filtration is further categorized into sieving, impaction, and diffusion depending on the size of the pollutant particles.[21] Electrical filtration works by inducing a charge on airborne particles, which are then attracted by the electric field.[22] The efficiency of filtration technology is evaluated by comparing the amount of particles in the air before and after passing through the filter.[23] In traditional filtration methods, high efficiency often results in pollutants adhering to the filter, which ultimately leads to a pressure drop, increased energy consumption, or a shorter filter lifespan. For this reason, next-generation filtration technologies must satisfy both efficiency and the conflicting factor of minimizing pressure drop simultaneously.

Herein, we classified indoor pollutants that negatively affect human health and explained next-generation air filtration technologies utilizing nanotechnology to effectively remove these pollutants (Fig. 1). Pollutants were broadly categorized into organic, inorganic, and biological pollutants, and we discussed how frequently each type of pollutant occurs in daily life, the transmission routes, and how they affect the human body. Next-generation air filtration technologies were explained in terms of fabrication processes, working principles, and their effectiveness against each type of pollutant. The electrospinning process was primarily used for the fabrication of next-generation filters, and we explained the principles and advantages of this process. The operating principles were divided into passive, self-powered, and active methods that utilize external power.

2. Sources of indoor air pollutants

Many indoor pollutants are generated from various sources, leading to a decline in IAQ. Indoor pollutants arise from dust, building materials, outdoor vehicle exhaust, smoking, cooking,

Hakbeom Lee is a PhD student in the Applied Nano and Thermal Science Lab, led by Prof. Seung Hwan Ko's group at Seoul National University, South Korea. He received his MS in the Department of Mechanical Engineering from Korea University in 2023 and a BS in the Department of Mechanical Engineering from Konkuk University in 2020. His current research focuses on the biosensors for molecule detection.

Hakbeom Lee

Seongmin Jeong is a Postdoctoral researcher in the Molecular Recognition Research Center at Korea Institute of Science and Technology (KIST), South Korea. He received his PhD in the Department of Mechanical Engineering from Seoul National University in 2024. His current research focuses on the nano-materials and process applied separation technology such as air purification system and breathable application.

Seongmin Jeong

Seung Hwan Ko is a Professor of Mechanical Engineering and Principal Investigator of the ANTS lab (https://ants.snu.ac.kr) at Seoul National University, South Korea. Before joining Seoul National University, he was a faculty member at KAIST, South Korea, since 2009. He received his PhD degree in mechanical engineering from UC Berkeley in 2006. He worked as a postdoctoral researcher at UC Berkeley until 2009. His current research interests include stretchable/flexible electronics, transparent electronics, soft robotics, wearable electronics, and laser-assisted nano/microfabrication.
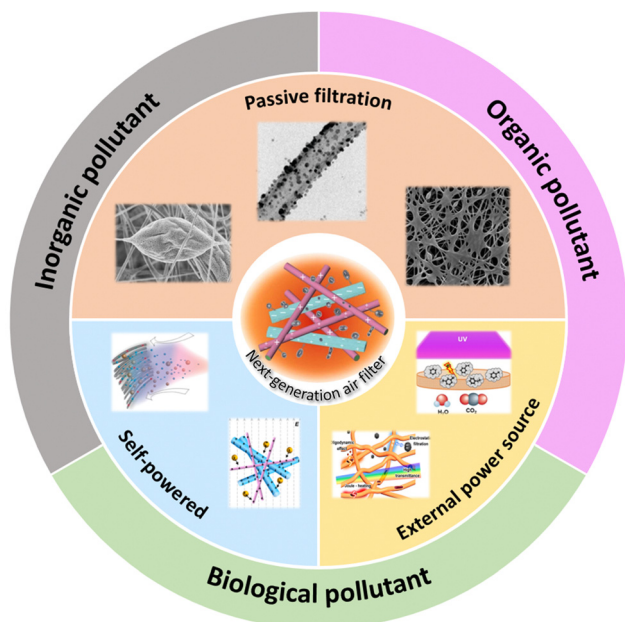
Seung Hwan Ko

Fig. 1 Schematic overview of next-generation air filtration technologies classified working principles and potential pollutants. (Reproduced with permission from ref. 24, Copyright 2016, American Chemical Society; Reproduced with permission from ref. 25, Copyright 2015, Elsevier; Reproduced with permission from ref. 26, Copyright 2011, American Chemical Society; Reproduced with permission from ref. 27, Copyright 2023, Elsevier; Reproduced with permission from ref. 28, Copyright 2021, Elsevier; Reproduced with permission from ref. 29, Copyright 2022, Wiley-VCH; Reproduced with permission from ref. 30, Copyright 2022, American Chemical Society; Reproduced with permission from ref. 31, Copyright 2022, Elsevier.).

and household products, entering the human respiratory system through inhalation. These pollutants come into contact with the respiratory mucous membranes, causing inflammatory reactions, alveolar damage, respiratory diseases, neurotoxicity such as headaches and confusion, and even carcinogenic effects. This issue is particularly significant for modern individuals who occupy over 90% of their time indoors. Additionally, airborne pathogens spread quickly in indoor spaces, leading to disease transmission, which can be especially fatal for immuno-compromised individuals. Therefore, it is crucial to be aware of the different types of pollutants that degrade IAQ and take preventive measures. Table 1 summarizes the toxicity and carcinogenicity of various air pollutants that affect human health.

2.1. Organic indoor air pollutants

Organic indoor air pollutants mainly consist of volatile organic compounds (VOCs), which, depending on their volatility and physical characteristics, can be classified as either VOCs or semi-volatile organic compounds (SVOCs). VOCs and SVOCs are gradually released indoors from building materials such as paints, adhesives, and flooring, as well as from cleaning and deodorizing products like disinfectants and air fresheners. They can also be released during combustion processes (smoking, cooking) and spread throughout the indoor air.[71,72] In addition, various VOCs are emitted from the skin or through respiration, making them an important consideration for IAQ.[73,74] Due to

their high volatility, VOCs exist in a vapor state and can easily be inhaled through the skin and respiratory system, leading to physiological dysfunctions in the nervous and respiratory systems, mutations, and cancer. Prolonged exposure to these compounds has been associated with the development of various cancers, including nasopharyngeal cancer, leukemia, lymphoma, and immune system disorders.[75,76] Additionally, respiratory diseases[77,78] such as asthma and bronchitis, as well as cognitive impairments related to neurodegeneration, have been observed.[79,80]

2.1.1. Volatile organic compounds (VOCs). Among the highly toxic VOCs are aromatic hydrocarbons, which include benzene, ethylbenzene, dichlorobenzene, xylene, styrene, toluene, and naphthalene. Their toxicological profiles can be reviewed through the Agency for Toxic Substances and Disease Registry (ATSDR), the U.S. Environmental Protection Agency (EPA), and the International Agency for Research on Cancer (IARC). Benzene (C_6H_6), used in products like paints, adhesives, and waxes, can cause respiratory effects like mucous membrane and nasal irritation, as well as blood-related effects, including leukopenia, anemia, and thrombocytopenia at concentrations over 60 ppm. At concentrations above 60 ppm, dermal and ocular irritation, central nervous system (CNS) depression, gastrointestinal, and cardiovascular effects have also been reported. Prolonged inhalation exposure can result in severe health conditions such as aplastic anemia, lymphoma, and leukemia. Benzene is recognized as a human carcinogen by the EPA (Group CH) and IARC (Group 1).[32] Ethylbenzene ($C_6H_5CH_2CH_3$), when inhaled, can cause severe throat, nasal, and ocular irritation at concentrations above 2000 ppm, along with hematological changes such as increased lymphocyte counts and decreased hemoglobin concentration. It can also cause neurological effects like nervous depression and ototoxicity (hearing loss). Although direct evidence of carcinogenicity in humans is lacking, studies on male rats have revealed renal tumors associated with the accumulation of $\alpha2\mu$-globulin in the epithelial cells of renal tubules. As a result, the IARC and EPA have classified ethylbenzene as Group 3 (inadequate evidence) and Group D (not classifiable), respectively.[33] Xylene (C_8H_{10}), composed of three isomers (m-xylene, o-xylene, p-xylene) and <20% ethylbenzene, can cause health effects that vary depending on the isomer. These effects include nose and throat irritation (mixed xylene at 200 ppm, m-xylene at 50 ppm, and p-xylene at 100 ppm), dizziness, tachycardia, hepatocellular vacuolation, and ocular effects. There is insufficient data on xylene's carcinogenicity in humans, so it has been classified by the EPA as Group InI (inadequate information to assess carcinogenic potential) and by IARC as Group 3.[34] Styrene ($C_6H_5CH{=}CH_2$), commonly used in plastic and resin manufacturing, is mainly inhaled and has been associated with upper respiratory tract irritation, nausea (376 ppm), decreased digestive function, increased stomach acidity (14 ppm), elevated γ-glutamyl transferase levels, elevated serum prolactin levels, eye irritation, and chronic vestibular–oculomotor system impairment. While styrene exposure has been linked to leukemia and lymphoma, the findings are limited due to concurrent exposure to multiple chemicals. IARC has categorized styrene as Group 2A, meaning it is likely carcinogenic to humans.[35] Toluene ($C_6H_5CH_3$), commonly found in paints, adhesives, and exhaust fumes, predominantly affects the nervous

Table 1 Health effects and Carcinogenicity of air pollutants in the indoor environment

	Pollutants			Health effects	Carcinogenicity (group)	Ref.
Organic	Volatile organic compounds	Aromatic hydrocarbon	Benzene (C_6H_6)	Respiratory irritation (60 ppm), leukemia, anemia, CNS depression, cancer	IARC (1) EPA (CH)	32
			Ethylbenzene ($C_6H_5CH_2CH_3$)	Respiratory irritation, hematological alterations (2000 ppm), nervous depression	IARC (3) EPA (D)	33
			Xylene ($(CH_3)_2C_6H_4$)	Nose/throat irritation, dizziness, tachycardia, hepatocellular vacuolation (100 ppm p-xylene)	IARC (3) EPA (InI)	34
			Styrene ($C_6H_5CH{=}CH_2$)	Respiratory irritation (376 ppm), digestive issues (14 ppm), vestibular/oculomotor impairment	IARC (2A)	35
			Toluene ($C_6H_5CH_3$)	CNS depression, cognitive disorder, respiratory irritation (50 ppm), cardiac arrhythmias, acidosis	IARC (3) EPA (InI)	36
			Naphthalene ($C_{10}H_8$)	Lung, nasal tumors, hemolysis, liver enlargement, jaundice, kernicterus	IARC (2B) EPA (C)	37
		Formaldehyde (CH_2O)		Respiratory irritation (5 ppm), chronic bronchitis (0.36 ppm), leukemia	IARC (1) EPA (B1)	38
		Trichloroethylene (C_2HCl_3)		Muscle necrosis, renal/liver cancer, dermal/ocular effects (200 ppm), non-Hodgkin's lymphoma	IARC (1) EPA (CH)	39
		Tetrachloroethylene ($Cl_2C{=}CCl_2$)		Respiratory irritation (216 ppm), dizziness (100 ppm), loss of vision, multiple myeloma	IARC (2A) EPA (LH)	40
		1,3-Butadiene ($C_4H{=}CH{-}CH{=}CH_2$)		Respiratory irritation, decreased hemoglobin/neutrophils (20 ppm), blood cancer, lymphoma	IARC (1) EPA (CH)	41
		Chloroform ($CHCl_3$)		CNS depression, lung damage (22 500 ppm), hepatitis, cardiac arrhythmia, cell necrosis (300 ppm)	IARC (2B) EPA (LH)	42
		2-Butanone (MEK; C_4H_8O)		Respiratory irritation (51–116 ppm), severe headache, dizziness, tachycardia	—	43
		Acrolein (CH_2CHCHO)		Asthma (0.6 ppm), hyperemia, necroses of the liver (305 ppm), diabetes	IARC (2A) EPA (InI)	44
		Acetone (C_3H_6O)		Respiratory irritation (500 ppm), CNS depression, renal effects, neuroblastoma	—	45
	Semi-volatile organic compounds	Chlorinated hydrocarbons	DDT ($C_{14}H_9Cl_5$)	Respiratory diseases, endocrine disruption, hematological effects, anti-androgenic effects	IARC (2A)	46
			Heptachlor ($C_{10}H_5Cl_7$)	Nervous system damage, hyperexcitability, tremors, convulsions, seizures	IARC (2B) EPA (B2)	47
			Chlordane ($C_{10}H_6Cl_8$)	Liver damage, liver tumors	IARC (2B) EPA (LH)	48
			Polychlorinated biphenyl ($C_{12}H_{10-x}Cl_x$)	CNS suppression, convulsions, bronchitis, sinusitis, respiratory diseases, cancer	IARC (1) EPA (B2)	49
		PAH	Benzo[a]pyrene ($C_{20}H_{12}$)	Respiratory diseases, lung cancer, DNA mutation, hepatomas	IARC (1) EPA (CH)	50
		PAE	Di(2-Ethylhexyl)Phthalate ($C_6H_4(CO_2C_8H_{17})_2$)	Testosterone reduction, pleural effusions, liver enzyme elevation, asthma, cancer	IARC (2B) EPA (B2)	51
Inorganic	Carbon oxide		Carbon dioxide (CO_2)	Headaches, cognitive decline, respiratory acidosis, inflammation	—	52–54
			Carbon monoxide (CO)	Hypoxia, dizziness, confusion, loss of consciousness, death	—	55,56
	Nitrogen oxide		Nitrogen dioxide (NO_2)	Airway inflammation, asthma, COPD, ischemic heart disease, lung cancer	—	57
			Nitrogen monoxide (NO)	Precursor for NO_2, contributes to ozone formation, respiratory irritation	—	57,58
	Reactive oxygen species		Ozone (O_3)	Ocular and respiratory irritation, cardiovascular diseases	IARC (3)	59,60
			Hydrogen peroxide (H_2O_2)	Ulcerative colitis, sepsis (558 μM), apoptosis	—	61
	Sulfur-compounds		Hydrogen sulfide (H_2S)	Respiratory diseases (COPD, lung cancer, asthma)	EPA (InI)	62
			Sulfur dioxide (SO_2)	Foul odor, neurological effects, eye irritation (15 mg m^{-3}), pulmonary edema	IARC (3)	63
	Particulate matter (PM)		PM$_{10}$ (Asbestos, Metals)	Upper respiratory issues, bronchitis, asthma	—	64
			PM$_{2.5}$ (SO_4^{2-}, NO_3^-, Metals)	Airway inflammation, asthma, COPD, lung infection	—	65
	Ammonia (NH_3)			Respiratory irritation, dermal/ocular burns, pulmonary edema	—	56,66
	Radon (Rn)			DNA damage of lung cells, lung cancer	IARC (1)	67
Biological	Airborne bacteria		Clostridium botulinum, *Bacillus anthracis*, etc.	Pneumonia, influenza, diarrhea, septicemia, respiratory infections	—	68–70
	Fungi and spores		*Blastomyces dermatitidis*, *Aspergillus niger*, etc.	Bronchitis, lung disease, diarrhea, septicemia, renal tumors	—	
	Virus		*Adenovirus*, *Herpes simplex virus*, *Measles*, etc.	Respiratory distress, abdominal cramps, pneumonia, gastroenteritis, viral hemorrhagic fevers, rash	—	

system, causing short-term effects like fatigue and headache, along with long-term effects such as cognitive and neuromuscular performance decline and hearing loss. Irritation of the eyes and nose (100 ppm), throat (50 ppm), and mucous membranes (48 ppm), along with cardiac arrhythmias, tachycardia, bradycardia, rhabdomyolysis, and acidosis due to renal malfunction have been reported. Despite its wide range of adverse effects on health, toluene is not classified as a direct carcinogen (Group 3 by IARC and Group InI by EPA).[36] Naphthalene ($C_{10}H_8$), used in deodorizers, dyes, and pesticides, has been shown to cause inflammation and damage to nasal and lung tissues, hemolysis, jaundice, anemia (patients with G6PD deficiency), liver enlargement, ocular effects, and immune suppression (decreased $CD8^+$ T cells) in infants. It has been associated with colorectal cancer in humans, and studies have shown a relationship with nasal and lung tumors in animals. Naphthalene is classified as Group 2B (IARC) and Group C (EPA) for possible human carcinogenicity.[37] Formaldehyde (CH_2O), a chemical often released from building materials, cleaning products, or incomplete combustion of carbon-containing materials, can be inhaled indoors and irritate the eyes, nose, and throat even at low concentrations of about 5 ppm, as well as bronchial inflammation and respiratory distress. Prolonged exposure has been linked to chronic bronchitis (0.36 ppm), lung damage, and various respiratory diseases. It has also been linked to renal failure, allergic contact dermatitis, and several cancers, including myeloid leukemia, nasopharyngeal cancer, and sinonasal cancer. Consequently, formaldehyde is classified as Group 1 (carcinogenic to humans) by IARC and Group B1 (likely human carcinogen) by the EPA.[38] Trichloroethylene (TCE; C_2HCl_3), commonly used in dry cleaning and as a solvent, has been linked to nausea, vomiting, anorexia (hepatosplenomegaly, hepatitis), muscle and liver necrosis, dermal and ocular irritation (200 ppm), as well as hepatobiliary cancers and non-Hodgkin's lymphoma. Prolonged exposure to TCE has been linked to a significantly increased risk of renal and liver cancers. TCE is recognized as carcinogenic by both the IARC (Group 1) and the EPA (Group CH).[39] Tetrachloroethylene (PERC; $Cl_2C=CCl_2$), used in paint removers, cleaning agents, and dry cleaning, can irritate the respiratory tract (216 ppm), dizziness, and urinary abnormalities suggesting mild tubular damage. The nervous system is particularly vulnerable, with symptoms including impaired coordination, anesthetic effects, depression (100 ppm), and loss of vision. Exposure to PERC has been linked to bladder cancer, multiple myeloma, and non-Hodgkin's lymphoma, resulting in its classification as Group 2A (IARC) and Group LH (likely human carcinogen) by the EPA.[40] 1,3-Butadiene ($C_4H=CH-CH=CH_2$), used in synthetic rubber production, enters the body mainly through inhalation and irritates the eyes, nasal passages, throat, and lungs. It has been associated with a decrease in hemoglobin, platelets, and neutrophils (20 ppm), weakening the immune system and increasing the risk of leukemia and lymphoma. Its potential to cause DNA mutations is currently under investigation. Given its strong association with genetic mutations and various blood cancers, 1,3-butadiene is classified as Group 1 (IARC) and Group CH (EPA).[41] Chloroform ($CHCl_3$), used in refrigerants, mold removers, and anesthetics, has well-documented health risks, leading to its restricted use.

Inhalation of chloroform vapors at high concentrations (22 500 ppm) can lead to CNS depression, lung damage, asphyxiation, cardiac arrhythmias, and renal failure. Extended exposure can lead to severe liver and renal damage (renal cell vacuolation (90 ppm), cell necrosis (300 ppm)), and animal studies have demonstrated a link to liver and renal cancers. As a result, chloroform is categorized as Group 2B by IARC and as a likely human carcinogen (Group LH) by the EPA.[42] 2-Butanone (MEK; C_4H_8O), used in solvents for cleaning agents, printing, and plastics, can irritate the upper respiratory tract, loss of appetite, gastrointestinal issues, and vision problems (51–116 ppm) when combined with methanol. Long-term exposure has been linked to chronic headaches, dizziness, tremors, and tachycardia. While MEK has been investigated for its potential link to oral and pharyngeal cancers, direct evidence of carcinogenicity is limited, and it has not been officially classified by IARC or the EPA.[43] Acrolein (CH_2CHCHO), generated through the incomplete combustion of petroleum, coal, and tobacco smoke, can cause asthma, nasal inflammation, bronchitis, and even liver damage at high concentrations. Exposure to acrolein can result in the production of harmful biomarkers (3-HPMA), which increases the risk of liver necrosis and hyperemia (305 ppm). It is also associated with skin and eye irritation, lateral medullary syndrome, and insulin resistance. Acrolein has shown a connection to rhabdomyoma and lung cancer in animal studies, resulting in its classification as Group 2A (probably carcinogenic) by IARC.[44] Acetone (C_3H_6O), commonly found in personal care products, including cleansing agents, perfumes, and hair or skin products, primarily causes respiratory (1000 ppm) and ocular irritation (500 ppm) and can lead to CNS depression and gastrointestinal hemorrhage in high concentrations. While studies have indicated a potential increase in neuroblastoma in children of parents exposed to acetone, there is insufficient evidence to classify it as carcinogenic. Acetone is not currently recognized as a carcinogen by IARC or the EPA, but long-term exposure may still cause significant health effects.[45]

2.1.2. Semi-volatile organic compounds (SVOCs). Although SVOCs have lower volatility than VOCs, their ability to gradually evaporate and attach to particulate matter in the air means they can be continuously inhaled or absorbed through the skin indoors. SVOCs include chlorinated hydrocarbons (CHCs), phthalic acid esters (PAEs), and polycyclic aromatic hydrocarbons (PAHs). Since these compounds are often found in products used indoors, prolonged exposure can lead to health issues in homes and workplaces. One such chlorinated hydrocarbon is dichlorodiphenyltrichloroethane (DDT; $C_{14}H_9Cl_5$), once widely used as a pesticide. Due to its harmful effects, including respiratory issues such as asthma, bronchitis, and hypersensitivity, DDT has been prohibited in many countries. DDT has been shown to cause liver enlargement, endocrine disruptions, and reduced sperm counts in men. Animal studies have indicated a link between DDT exposure and higher rates of liver cancer, and IARC classified it as Group 2A (likely carcinogenic to humans).[46] Another chlorinated hydrocarbon, Heptachlor ($C_{10}H_5Cl_7$), used for termite control, has a long-lasting presence in soil, water, and the fatty tissues of animals.

Heptachlor has been associated with neurological damage, tremors, convulsions, and hyperexcitability. It is also linked to malformations in fetuses exposed to it during pregnancy, as well as immunosuppression. Heptachlor exposure is associated with breast cancer and non-Hodgkin's lymphoma, and it falls under the Group 2B classification by IARC and Group B2 by the EPA.[47] Chlordane ($C_{10}H_6Cl_8$), chemically similar to heptachlor, has similar adverse effects, such as liver damage and the potential to cause liver tumors in animal studies. Chlordane is classified as Group 2B by IARC and Group LH by the EPA.[48] Polychlorinated Biphenyls (PCBs; $C_{12}H_{10}$–xCl_x), widely used in electrical insulators, lubricants, and coolants, have 209 isomers and are extremely stable, leading to persistent environmental accumulation. PCBs have been linked to CNS suppression, headaches, dizziness, and muscle tremors, as well as chronic bronchitis and sinusitis. When inhaled at high concentrations, PCBs can cause aplastic anemia, hemolytic anemia, and thrombocytopenic purpura. Prolonged occupational exposure has been associated with liver cancer and lymphoma, and PCBs are classified as Group 1 by IARC and Group B2 by the EPA.[49] Benzo[a]pyrene (BaP; $C_{20}H_{12}$), a type of polycyclic aromatic hydrocarbon (PAH), is generated through the incomplete combustion of coal, oil, wood, and tobacco. It is highly carcinogenic and has been associated with respiratory irritation, bronchovascular markings, pleural effusions, and lung cancer. BaP exposure can lead to adenomas, hepatomas, and immune suppression. IARC classified BaP as Group 1, and the EPA classified it as Group CH (carcinogenic to humans) and also developed an evaluation system known as "m-rpf" to assess the relative potency of carcinogenicity and mutagenicity, with BaP serving as the benchmark for assessing other substances' carcinogenic potential.[50] Di(2-Ethylhexyl)Phthalate (DEHP; $C_6H_4(CO_2C_8H_{17})_2$), utilized as a plasticizer in products like vinyl flooring and packaging materials, can be ingested orally, causing adverse health effects. Prolonged exposure to DEHP has been associated with nausea, vomiting, headaches, liver enzyme increases, reduced testosterone levels, fetal developmental disorders, and asthma. Prolonged low-level exposure can lead to breast, prostate, and thyroid cancers, and DEHP is classified as Group 2B by the IARC and Group B2 by the EPA.[51]

2.2. Inorganic indoor air pollutants

With growing recognition of the importance of IAQ, much attention has been paid to the risks associated with indoor organic pollutants. However, due to several factors such as the rise in particulate matter caused by environmental pollution, increased indoor population density and time spent indoors, and the growing diversity of indoor emission sources, indoor inorganic pollutants are also receiving significant attention. Inorganic substances are often naturally generated through human respiration, combustion, indoor activities, the use of various chemical products, and airborne chemical reactions. Since these pollutants primarily contribute to respiratory diseases, indicators such as particulate matter (PM), CO_2, and NO_x are frequently used to assess and improve IAQ.

Examples of carbon oxides include carbon dioxide (CO_2) and carbon monoxide (CO). CO_2 is released through human respiration (7.5 L s^{-1} per person) and combustion processes, with a threshold range of 700–1500 ppmv, and it is recommended to keep indoor CO_2 concentrations below 700 ppmv.[81] Additionally, CO_2 serves not only as a key indicator of IAQ but also as a marker for the spread of the SARS-CoV-2 virus, which causes COVID-19.[82] Exposure to CO_2 can cause headaches and reduced cognitive ability and long-term exposure to levels around 3000 ppm may lead to respiratory acidosis, increased inflammatory responses, metabolic syndrome, and bone demineralization.[52–54] CO, a colorless and odorless gas, is emitted during the incomplete combustion of carbon-based fuels (e.g., gasoline, tobacco, wood) and poses a significant toxic threat to humans. The WHO includes CO among its selected indoor pollutants to highlight its danger.[67] The exposure limit for CO is set at 4 mg m^{-3},[58] and exposure to elevated levels can lead to hypoxia, leading to headaches, dizziness, confusion, and, in severe cases, loss of consciousness or death.[55,56] Nitrogen oxides (NO_x) comprise nitrogen dioxide (NO_2) and nitric oxide (NO), both of which are mainly produced through combustion processes in kitchens, tobacco smoke, kerosene heaters, and outdoor vehicle exhaust. NO_2, which can also form through the oxidation of NO with oxidants, is five times more toxic than NO and is listed by the World Health Organization (WHO) as one of its selected indoor pollutants, with an exposure limit of 25 μg m^{-3} for 24 hours.[58,83] NO_2 is highly reactive and can react with VOCs to form ozone (O_3), serving as a precursor to further pollution, which requires careful concentration control. Short-term exposure to NO_2 can cause airway inflammation, bronchoconstriction, and asthma, while long-term exposure increases the risk of chronic obstructive pulmonary disease (COPD), respiratory infections, diabetes, ischemic heart disease, and lung cancer, potentially leading to death.[57] Many countries have recognized the severity of NO_x and have implemented policies to limit emissions.[56,83] Examples of Reactive Oxygen Species (ROS) include ozone (O_3) and hydrogen peroxide (H_2O_2). Both are strong oxidizing agents that effectively oxidize pollutants, offering antimicrobial benefits, but they can also react with other substances to form secondary pollutants.[84] Ozone is generated in the atmosphere by ultraviolet radiation and is emitted indoors from air purifiers, washing machines, photocopiers, and printers. Due to its strong oxidative properties, ozone can cause ocular and dermal irritation, and high exposure levels can lead to cardiovascular diseases, including ischemic heart disease and hypertension.[59,60] Ozone is included in the WHO's selected indoor pollutants, with a recommended exposure limit of 100 μg m^{-3} for 8 hours.[58] Hydrogen peroxide is naturally produced in the body and can accumulate indoors from sterilizers and air purifiers. Excessive accumulation (30 μM) has been linked to ulcerative colitis, sepsis (558 μM), apoptosis, cellular damage, and organ dysfunction.[61] Sulfur dioxide (SO_2) and hydrogen sulfide (H_2S) are both sulfur-containing gases primarily generated through the combustion of fuels used for cooking and heating. SO_2 is a colorless, toxic gas with a pungent, irritating odor, and it can cause respiratory diseases, including COPD, lung cancer, and childhood asthma.[63] The WHO has selected SO_2 as an indoor pollutant, with a recommended exposure limit of 40 μg m^{-3} for

24 hours.[58] H_2S, another pollutant with a foul odor, can originate from sulfur-containing groundwater, septic tanks, and landfill gas emissions.[56] Low-level H_2S exposure can cause headaches, neurological symptoms, and eye irritation at concentrations around 15 mg m^{-3}, while high concentrations can lead to pulmonary edema. The WHO recommends a day average exposure limit of 150 µg m^{-3}.[62] PM is categorized into PM$_{2.5}$ and PM$_{10}$ based on particle size. These particles are primarily generated by exhaust fumes, cooking, heating, tobacco smoke, road dust, and construction sites. As key indicators of IAQ, the WHO includes particulate matter in its selected indoor pollutants, with recommended 24-hour average concentrations of 15 µg m^{-3} for PM$_{2.5}$ and 45 µg m^{-3} for PM$_{10}$.[58] PM$_{2.5}$ particles, measuring less than 2.5 µm in diameter, contain substances such as sulfates (SO_4^{2-}), nitrates (NO_3^-), ammonium (NH_4^+), and metals (Pb, Cd, Ni, Cu, Zn) (VOCs are also included but have been discussed earlier and are therefore omitted here).[85] Because of their small size, PM$_{2.5}$ particles can reach deep into the lungs, causing airway inflammation, asthma, COPD, cell death due to respiratory infections, and autophagy.[64] PM$_{10}$ particles, which are larger than 10 µm, contain substances such as asbestos, minerals (Al, Ca, Fe, Mg, K, Si, Ti), dust, metals, and water-soluble ions.[65] PM$_{10}$ particles, due to their larger size, affect the upper respiratory system and can cause bronchitis, asthma, and other respiratory diseases. Ammonia (NH_3) is released from fertilizers, vehicle exhaust, cooking combustion, tobacco smoke, human respiration, and urine and feces. Indoor ammonia concentrations tend to be 10 times higher than outdoor levels (indoor: 10–70 ppb; outdoor: 50 ppt–5 ppb).[86] The U.S. Occupational Safety and Health Administration (OSHA) sets the indoor ammonia exposure limit at 25 ppm for 8 hours.[87] High concentrations of NH_3 can irritate the upper respiratory tract, cause chemical burns and edema in exposed tissues, and lead to breathing difficulties and pulmonary edema.[56,66] Radon (Rn) is a naturally existing, colorless, and odorless radioactive gas. It originates from the decay of uranium (U) or radium (Ra) in rocks and can enter indoor spaces through groundwater. Due to its radioactive nature, long-term radon exposure can result in radiation exposure, which can damage lung cell DNA and lead to lung cancer.[67] The risks of radon have been widely reported, and the IARC categorizes it as a Group 1 carcinogen. The WHO also includes radon in its selected indoor pollutants, recommending that indoor radon levels not exceed 100 Bq m^{-3}.

2.3. Biological indoor air pollutants

The COVID-19 pandemic significantly changed our understanding of IAQ and its health effects. While attention had traditionally focused on VOCs and inorganic pollutants outdoors, the pandemic highlighted the importance of biological air pollutants. The realization that pathogens like the SARS-CoV-2 virus can float freely in densely populated indoor spaces and easily transmit between people has emphasized the need for ventilation and air purification.[88,89] This shift in perspective has underscored the effect of IAQ on health, especially in the everyday spaces where people spend time.

Studies have explored the size, concentration, and variety of biological particles present in indoor environments, identifying bioaerosols as key sources of transmission and infection between humans.[90–92] While bioaerosols themselves are not directly toxic to humans, they can cause various pathological conditions through infections and allergic reactions. Bioaerosols emitted by infected individuals are primarily composed of airborne bacteria, fungi and spores, and viruses.[93,94] Bioaerosols are classified into droplet transmission and airborne transmission based on particle size of 5 µm. Droplets exceeding 5 µm in size usually settle on surfaces within approximately 90 cm (3 feet) far from the infected person, leading to direct transmission. In contrast, aerosols smaller than 5 µm can stay airborne for several hours to days, facilitating airborne transmission and making them more dangerous.[95–99] Pathogens are emitted from infected individuals through various routes, including (1) sneezing (40 000 particles per sneeze), (2) toilet flushing (20 000 particles per flushing), (3) vomiting (1000 particles per event), (4) coughing (710 particles per cough), and (5) talking (36 particles/100 words).[95] Bartlett *et al.* found that pathogen particles released indoors were present at a concentration of geometric mean (GM): 227 CFU m^{-3}, nine times higher than the outdoor concentration of GM: 26 CFU m^{-3}. Additionally, natural ventilation (GM: 324 CFU m^{-3}) resulted in twice the concentration of bioaerosols compared to mechanical ventilation (GM: 166 CFU m^{-3}), underscoring the importance of ventilation and the impact of bioaerosols on IAQ.[100]

Pathogens can invade the body through inhalation or skin contact, infecting various organs and causing severe health problems.[68–70] The following are some examples of major pathogens and the diseases they can cause: For bacteria, pathogens such as *Bordetella pertussis, Legionella pneumophila, Mycoplasma, Neisseria meningitidis, Staphylococcus aureus,* and *Streptococcus pneumoniae* can cause respiratory symptoms such as pneumonia, influenza, and infections.[68–70] *Escherichia coli* and *Staphylococcus epidermidis* can cause gastrointestinal effects like gastroenteritis, diarrhea, and food poisoning.[68] *Micrococcus luteus* and *Neisseria meningitidis* can cause meningitis, while *Pseudomonas fluorescens* and *Staphylococcus aureus* can lead to septicemia.[68,70] For fungi and spores, pathogens like *Blastomyces dermatitidis* and *Histoplasma capsulatum* can cause respiratory diseases such as bronchitis and chronic lung disease.[68,69] *Aspergillus versicolor* can lead to gastrointestinal symptoms such as gastroenteritis, abdominal cramps, diarrhea, and vomiting, while *Penicillium spinulosum* can cause septicemia.[68] *Penicillium citrinum* has been linked to renal tumors, and *Aspergillus niger* can cause ear infections, sore throats, and skin infections.[68] For viruses, pathogens such as *Adenovirus, Avian influenza, MERS-CoV, Rhinovirus,* and *SARS-CoV* can cause respiratory effects, including acute respiratory distress, pneumonia, and pulmonary infections.[68–70] *Adenovirus, Enteric viruses, Norovirus,* and *Rotavirus* can cause gastrointestinal effects such as abdominal cramps, diarrhea, and gastroenteritis.[68–70] Pathogens like *Ebola virus, Marburg virus, Crimean-Congo fever virus,* and *Lassa virus* can cause viral hemorrhagic fevers, while *Herpes simplex virus, Measles, Varicella-zoster virus,* and *Variola virus* can cause rash or exanthems, chickenpox, and other symptoms.[68–70]

As pathogens continually evolve and mutate, new ones are still being discovered, rendering them a continual focus of ongoing research. The global pandemic, which has resulted in

over 600 million deaths,[88,89] has heightened awareness of bioaerosols and underscored the need for continuous IAQ research, particularly regarding biological pollutants.

3. Next-generation air filtration

3.1. Nanofabrication process for air filtration

The performance of the air filter can be described by the quality factor (QF), which is the ratio of two conflicting factors: filtration efficiency and pressure drop.[101] As the surface area of the air filter increases, the probability of pollutants adhering to the filter *via* mechanical filtration mechanisms also increases, thereby enhancing filtration efficiency. Plus, as the porosity increases, the pressure drop decreases. Therefore, to manufacture high-performance filters, a thin fibrous structure with a high surface-to-volume ratio and high porosity is required. The fiber manufacturing process results in the creation of networking between the fibers, which can be classified into woven fabric and nonwoven fabric depending on the type of networking. Woven fabric has a tightly packed and regular grid structure, resulting in a very low surface-to-volume ratio and porosity.[102] Hence, to achieve high air permeability and filtration efficiency at the same time, various processes are used to form nonwoven fabric, which enables the production of high-performance filters.

3.1.1. Traditional processes. Many processes are used for manufacturing air filters, with the most representative being the melt-blown process. This process involves blowing hot air into a polymer solution to produce nonwoven fabric, and it is the method currently used to manufacture most commercial masks and industrial filters.[103] While it has the advantage of allowing mass production of filters with large sizes at low cost, it has drawbacks such as difficulty in precisely controlling factors that can affect filter performance, such as fiber diameter, pore size, and distribution, along with lower mechanical strength.

Another process capable of producing nonwoven fabric is the spunbond process. This process involves melting thermoplastic synthetic resin at high temperatures and uniformly extruding it into filaments, which are then solidified to form fibers.[104] The advantages of this method include a simple manufacturing process and the ability to produce the final product directly from raw resin in a single step. It also offers high mechanical strength and is widely used in the production of many commercial products. However, the drawback is that the fiber diameter is relatively large, making it difficult to filter very fine particles.

Another nonwoven fabric manufacturing process is the flash spinning process. In this process, a mixture of polyolefin resin and solvents like Freon gas is created under high temperature and high-pressure conditions, resulting in a supercritical fluid state. The mixture is then rapidly extruded into an environment at normal temperature and pressure, where the temperature and pressure differences are used to create ultrafine fibers through high-speed stretching.[105,106] The fibers produced through this process exhibit excellent strength and uniform structure; however, the complexity of the equipment, the high cost of the process, and the limitations on usable materials are significant drawbacks.

3.1.2. Electrospinning process. Electrospinning is a process that produces thin and long nanofibers by utilizing the stretching and elongation of solution droplets at the tip of a charged needle nozzle, driven by electrostatic repulsion. The electrospinning process generally involves four sequential stages: (i) charging the solution droplet and making a Taylor cone (a conical jet); (ii) stretching the charged jet in a straight trajectory; (iii) the jet undergoes thinning due to the effects of an electric field, accompanied by the development of electrical bending instability, also referred to as whipping instability; and (iv) the jet solidifies and is deposited as solid fibers onto a grounded collector[107] (Fig. 2a). The components used in this process include a high-voltage power supply, a syringe pump, a needle nozzle, and a grounded conductive collector (Fig. 2b). Due to its simplicity in components and operation, this process is widely used for both experimental and commercial purposes. The nanofibers produced through the electrospinning process form a nonwoven fabric, and unlike traditional fiber manufacturing methods, they can uniformly produce fibers with diameters of a few tens of nanometers and long lengths (Fig. 2c–e). This allows the filtration of much smaller particles and provides a high surface-to-volume ratio and high porosity at the same time.[108] Therefore, electrospinning is suitable for producing next-generation filters with a high QF, and many studies have adopted this process.[109–113]

The electrospinning process primarily uses organic polymer-based solutions. Therefore, many electrospun (e-spun) nanofibers offer relatively flexible production forms and can possess biocompatible properties. In addition to this, fibers can also be produced using solutions composed of various materials such as small molecules,[117–119] colloidal particles,[120,121] and composites,[122–124] allowing for the modification of filter characteristics and enabling the creation of air filters specialized for specific pollutants. In addition to the composition of the solution, different process parameters, including the concentration and viscosity of the solution, the intensity of the electric field, and the distance between the nozzle tip and the conductive collector can be adjusted to easily achieve precise filter characteristics, such as porosity. Another advantage of the electrospinning process is that it allows for a multi-nozzle system, which can significantly increase productivity and enable the continuous deposition of immiscible material.[125] By modifying the multi-nozzle process, it is possible to create a core/shell structure.[126] The main advantage of the core/shell structure is that it allows for the use of multiple materials within a single fiber, enabling the creation of multifunctional filters that effectively remove various pollutants while maintaining strong mechanical properties. For instance, in the study by Liu *et al.*, the shell material polar polymer Nylon-6, which is excellent at adsorbing pollutants, was used, and the core material flame retardant triphenyl phosphate (TPP) was included. In the event of a fire, the shell melts, releasing the flame retardant from the core, allowing the filter to extinguish the fire immediately.[127]

3.2. Working principles of air filtration

To address the limitations of traditional commercial filters, nanotechnology-enhanced filters improve the material or

structural properties of fibers, resulting in higher filtration efficiency and new functionalities. These filters can achieve energy-efficient pollutant filtering or monitoring through self-powering mechanisms, and by utilizing external power sources, they can enhance efficiency through new filtration mechanisms.

3.2.1. Passive filtration. Passive filtration primarily relies on mechanical filtration mechanisms enabled by nanostructures. When the size of the pollutant exceeds 200 nm, sieving and inertia of mechanical filtration mechanisms become the dominant processes. Pollutants traveling with air adhere to the filter material, allowing clean air to pass through the lower part of the filter. To prevent blocking of the filter pores and the resulting pressure drop, research has been conducted to modify the filter's structure. Most nanofibers are produced using the electrospinning process, which creates thin diameters and filters contaminants through mechanical filtration mechanisms. Matulevicius *et al.* reported the effects of various factors in the electrospinning process, such as polymer concentration, solvent ratio, process time, distance between the nozzle tip and the conductive collector, and operating voltage, on the diameter, morphology, basis weight, and thickness of nanofibers. Through process optimization, they produced an ultrafine nanofiber filter with a small fiber diameter of 62 nm, high filtration efficiency of 90.9%, and an excellent QF.[128] Souzandeh *et al.* enhanced the filtration performance by denaturing soy protein to form numerous functional groups on its surface, mixing it with polyvinyl alcohol (PVA), and producing fibers through the electrospinning process, thereby increasing interactions with various pollutants (Fig. 3a). Soy protein, which is abundant and low-cost, naturally contains ionizable groups such as glutamic acid, lysine, and histidine, which can provide an active area to capture bacteria. Additionally, these ionizable groups provide the advantage of capturing pollutants with up to 99.80% efficiency through an electric filtration mechanism. The nanofiber filter produced through this process not only exhibits excellent chemical interaction with small particulate matter but also demonstrates strong performance in capturing molecular VOCs, achieving up to 90.90% efficiency. In this study, the optimal performance was observed when the soy protein to PVA ratio was 1:1, and the areal density of the filter was 4.5 g m^{-2}.[24] Studies that modified the fiber structure to alter filtration efficiency have also been reported. Zhang *et al.* adopted a modified electrospinning process known as capacitive-like electronetting to form continuous 2D nanonetworks in large quantities (Fig. 3b). Filters with this structure exhibit multifunctionality, being effective for both rigid solid and soft oil particles. This study achieved up to 99.98% PM removal efficiency with 95% transparency.[129] Wang *et al.* reported a study where bead-like structures were generated between nanofibers using the electrospinning process (Fig. 3c). By modifying the concentration of the polylactic acid (PLA) solution and the ratio of the solvents dichloromethane (DCM) and *N*,*N*-dimethylacetamide (DMAC), the researchers were able to control the diameter of the nanofibers and the size of the beads. This bead-on-string structure contributed to decreasing the density of the fibers and increasing the distance between them, leading to a reduced pressure drop in the filter. Additionally, the thin nanofibers with a diameter of

143.8 nm and the nanopores on the bead surface provided significant advantages in capturing fine particles.[25] Li *et al.* fabricated e-spun polyvinylidene fluoride (PVDF) nanofibers with a diameter of approximately 40 nm and a mean pore size of 100–200 nm through the Steiner geometrical structure. Throughout the electrospinning process, anionic surfactant was added to the PVDF solution, which induced a phase change from the α-phase to the β-phase, enhancing the electrostatic force and improving interactions with pollutants. The filter using the Steiner structure exhibited a filtration efficiency of up to 99.985% and a low pressure drop of 66.7 Pa.[130] In addition to the filtering role of nanofibers, studies have also explored new functionalities. Liu *et al.* fabricated nanofibers using various readily available polymers and noted that the extent of PM adsorption varied depending on the dipole moment of the polymer (Fig. 3d). The filters maintained a high transparency of over 90% while achieving more than 95% filtration efficiency. Utilizing these properties, they developed an energy-efficient air filter window that can be directly attached to windows.[131] It has been reported that when silver, metal oxides, or carbon composites are used in air filters, they inhibit bacterial DNA replication, leading to excellent antibacterial effects.[132–134] Jung *et al.* formed Ag/carbon nanotube (CNT) hybrid nanoparticles (NPs) (ACHNPs) by embedding AgNPs uniformly onto CNTs produced through aerosol nebulization and thermal processes. These ACHNPs were evenly deposited onto a polyurethane (PU) filter, demonstrating superior antimicrobial effects compared to filters using only AgNPs or CNTs, while also maintaining a low pressure drop (Fig. 3e).[26] Ko *et al.* mass-produced AgNP@SiO$_2$ hybrid particles (ASHPs) by growing AgNPs on aminopropyl-functionalized silica colloids as a support material. After coating ASHPs onto a glass fiber filter, it was confirmed that they exhibited long-term antibacterial effects. Bacterias were used for performance evaluation, and at an areal density of 10^8 particles per cm^2, the filter demonstrated a removal efficiency of 99.99% for both types of bacteria.[135] Protein-based nanofibers are also known for their excellent antibacterial properties. Souzandeh *et al.* fabricated protein-based nanofibers through the electrospinning process, enabling effective interactions with pollutants through various functional groups. They developed an environmentally friendly nano-filter by adding a cross-linking agent, which exhibited excellent antimicrobial effects and remained stable in various environments, including humidity levels above 95%.[136] Non-fiber filters have also been reported. Jung *et al.* formed reduced graphene oxide (rGO) foam attached to both sides of a copper mesh using ion-mediated assembly. The rGO foam, with its porous property and high surface area, removes pollutants from indoor and outdoor air at the same time. The filter used in this study is washable and reusable, exhibiting a high PM$_{2.5}$ removal efficiency of 99.9% with a low pressure drop of 5 Pa. Graphene's unique combination of high electrical conductivity, chemical stability, and large surface area makes it highly effective in adsorbing and trapping fine PM$_{2.5}$, a major contributor to air pollution with severe health impacts.[137] Zhao *et al.* used a chemical vapor deposition (CVD) process to grow multi-walled CNTs (MWCNTs) on a porous alumina ceramic membrane, significantly increasing the surface area and achieving a
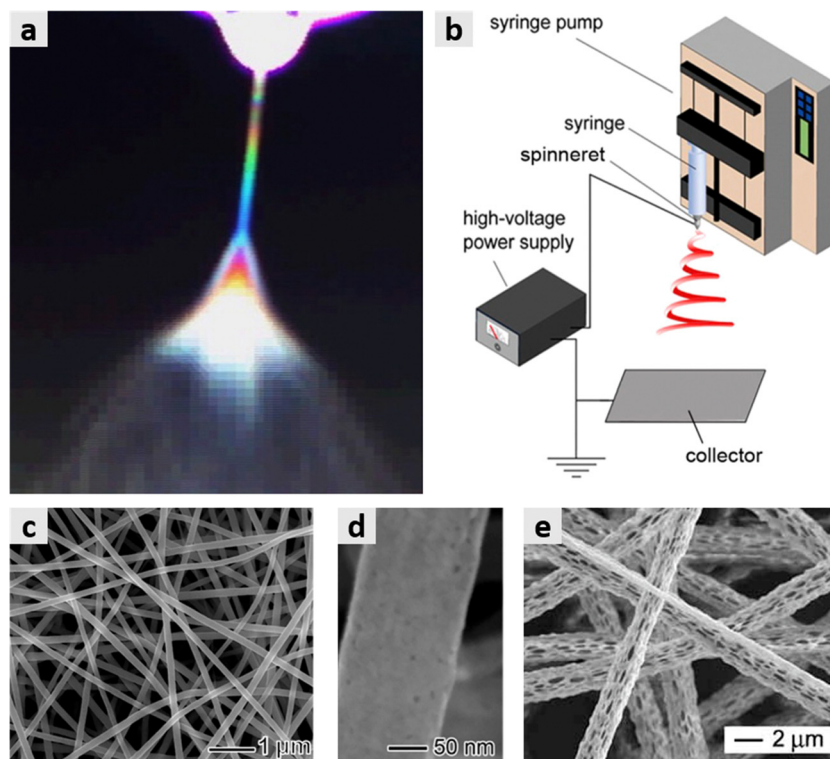
Fig. 2 (a) A digital image of the Taylor cone and thinning jet of solution. (Reproduced with permission from ref. 114, Copyright 2008, Elsevier). (b) Schematic of setup for electrospinning process. (Reproduced with permission from ref. 115, Copyright 2017, American Chemical Society). (c)–(e) SEM images of various e-spun fibers. (Reproduced with permission from ref. 115, Copyright 2017, American Chemical Society; Reproduced with permission from ref. 116, Copyright 2008, Wiley-VCH).

remarkable filtration efficiency of 99.9999%. The filter exhibited a 62.9% lower pressure drop compared to the pristine filter. MWCNTs damage the bacterial cell wall and then penetrate the cell, inhibiting cell division. As a result, the filter demonstrated excellent antibacterial effects, with an efficiency of 97.86%, along with high durability.[138]

3.2.2. Self-powered filtration. If the size of the pollutant is below 200 nm, diffusion of mechanical filtration mechanisms becomes the dominant mechanism. Small particles can be effectively captured by utilizing the electrical filtration mechanism, which leverages the electrical charge on particles to create an attractive force. Self-powered filtration systems generate an electrical filtration mechanism that can operate simultaneously with mechanical filtration, thereby improving overall filtration efficiency. Filters utilizing self-powering mechanisms mostly rely on the triboelectric effect. The triboelectric effect occurs when electrons move between two materials with different electrical properties during contact, causing each material to carry a charge upon separation.[139] Materials such as polytetrafluoroethylene (PTFE) and PVDF, which easily gain electrons, or polypropylene (PP) and Nylon, which easily lose electrons, are commonly used. Since an electric field can be generated through simple mechanical movements, this allows for additional electrical filtration on the surface of nanofibers. Bai *et al.* demonstrated that a five-layer structure composed of PTFE and Nylon fabrics can generate static electricity through friction, achieving a particle removal efficiency of up to 96% for $PM_{2.5}$ particles. This performance

was approximately 1.39 times higher than when the filter was not charged. The filter also exhibited a high filtration efficiency of 84.7% for very small particles such as $PM_{0.5}$, and it maintained its high-performance electrostatic filtration even after multiple washes.[140] Hu *et al.* demonstrated that by combining UiO-66 metal–organic frameworks (MOFs) with PVDF to create tribo-electric e-spun fibers, they achieved a voltage of 52.8 V, a current of 4.29 μA, and a transferred charge of 22.02 nC, which represents improvements of 6.5 times, 5.1 times, and 8.0 times, respectively, compared to using PVDF alone. Additionally, the filter showed an efficiency of nearly 98% for $PM_{2.5}$ and maintained almost the same performance after four washes. MOFs, with their high surface area, adjustable pore sizes, and abundant active sites, significantly enhance the electrostatic and physical capture of fine PM, a key air pollutant with severe health impacts.[141] Wang *et al.* reported a "self-charging triboelectric air filter" (S-TAF) that generates positive and negative charges through the friction between PTFE fibers with surface cracks, designed to maximize surface area, and core/shell PP/polyethylene (PE) fibers (Fig. 4a). S-TAF, with its unique core/shell structure, exhibits very high porosity and large pore size, achieving a high filtration efficiency of 99.28% and an exceptionally low pressure drop of 26.46 Pa, while maintaining long-term stability.[27] Wang *et al.* significantly enhanced the triboelectric effect by layering polyacrylonitrile (PAN) fibers and PP fibers coated with poly(3,4-ethylenedioxythiophene:poly(styrenesulfonate) (PEDOT:PSS) on one side. The filter demonstrated consistent filtration efficiency of 94% for
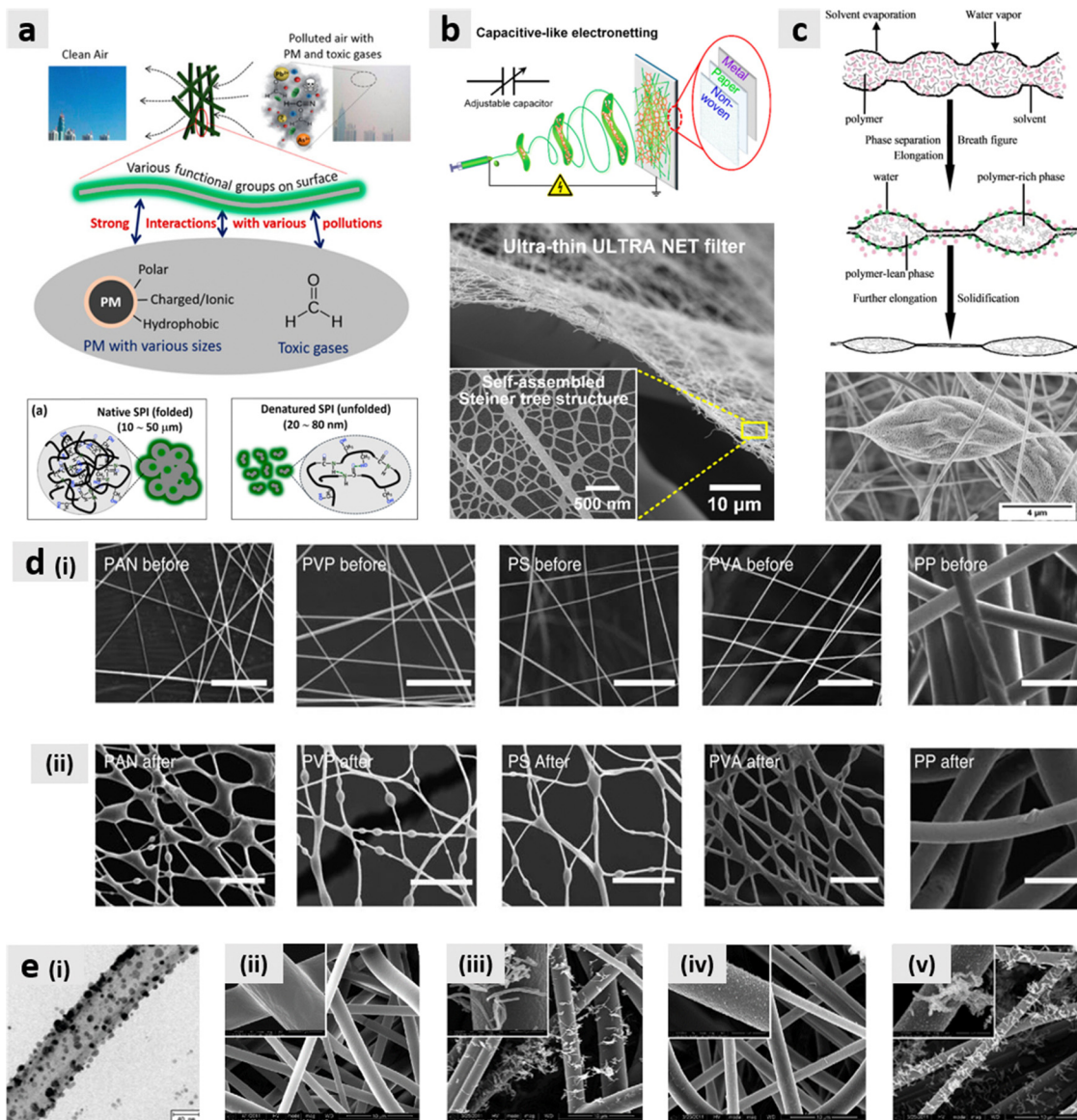
Fig. 3 (a) Protein-based nanofabrics for multifunctional filtration. (Reproduced with permission from ref. 24, Copyright 2016, American Chemical Society). (b) Schematic of ultra-thin fiber with capacitive-like electronetting process and its SEM image. (Reproduced with permission from ref. 129, Copyright 2019, American Chemical Society). (c) Schematic and SEM image of bead-on-string structure formation in PLA fibers. (Reproduced with permission from ref. 25, Copyright 2015, Elsevier). (d) SEM images of various polymer filters (i) before filtration, (ii) after filtration. (PVP: polyvinylpyrrolidone, PS: polystyrene) Scale bars in (d) and (e) 5 μm. (Reproduced with permission from ref. 131, Copyright 2015, Springer Nature). (e) SEM images of (i) ACHNPs, (ii) Pristine filter, (iii) CNT-deposited filter, (iv) Ag-nanoparticle-deposited filter, (v) ACHNPs-deposited filter. (Reproduced with permission from ref. 26, Copyright 2011, American Chemical Society).

particles sized 0.3–0.4 μm and 99% for particles sized 1–2.5 μm over 48 hours. The filter also showed a very low pressure drop of 110 Pa and exhibited sterilization performance against viruses through Ag nanowire (NW) coating.[28] Self-powered mechanisms not only improve filtration efficiency but also enable data collection for monitoring. He *et al.* reported a triboelectric smart filter (TSF) capable of collecting data including respiratory rate, inhalation time, and exhalation time. As the contact area of the PAN and PVDF nanofibers changes with breathing, the triboelectric effect causes PAN to lose electrons, while PVDF gains electrons, forming a negative charge and creating a voltage difference (Fig. 4b).

Respiratory signals were stably measured for over 40 hours, and the TSF demonstrated a filtration efficiency of 99% for particles sized 0.3–0.5 μm. TSF maintains high porosity and low pressure drop due to the fine pore structure of the PAN and PVDF nanofiber layers.[142] Another self-powered principle is the piezoelectric effect. The piezoelectric effect occurs when a material with piezoelectric properties undergoes mechanical deformation, causing changes in its crystal structure and resulting in a redistribution of internal charges, which creates an electric field.[143] Materials like quartz, lead zirconate titanate (PZT), PVDF, and PLA are commonly used piezoelectric materials. Zhang *et al.*
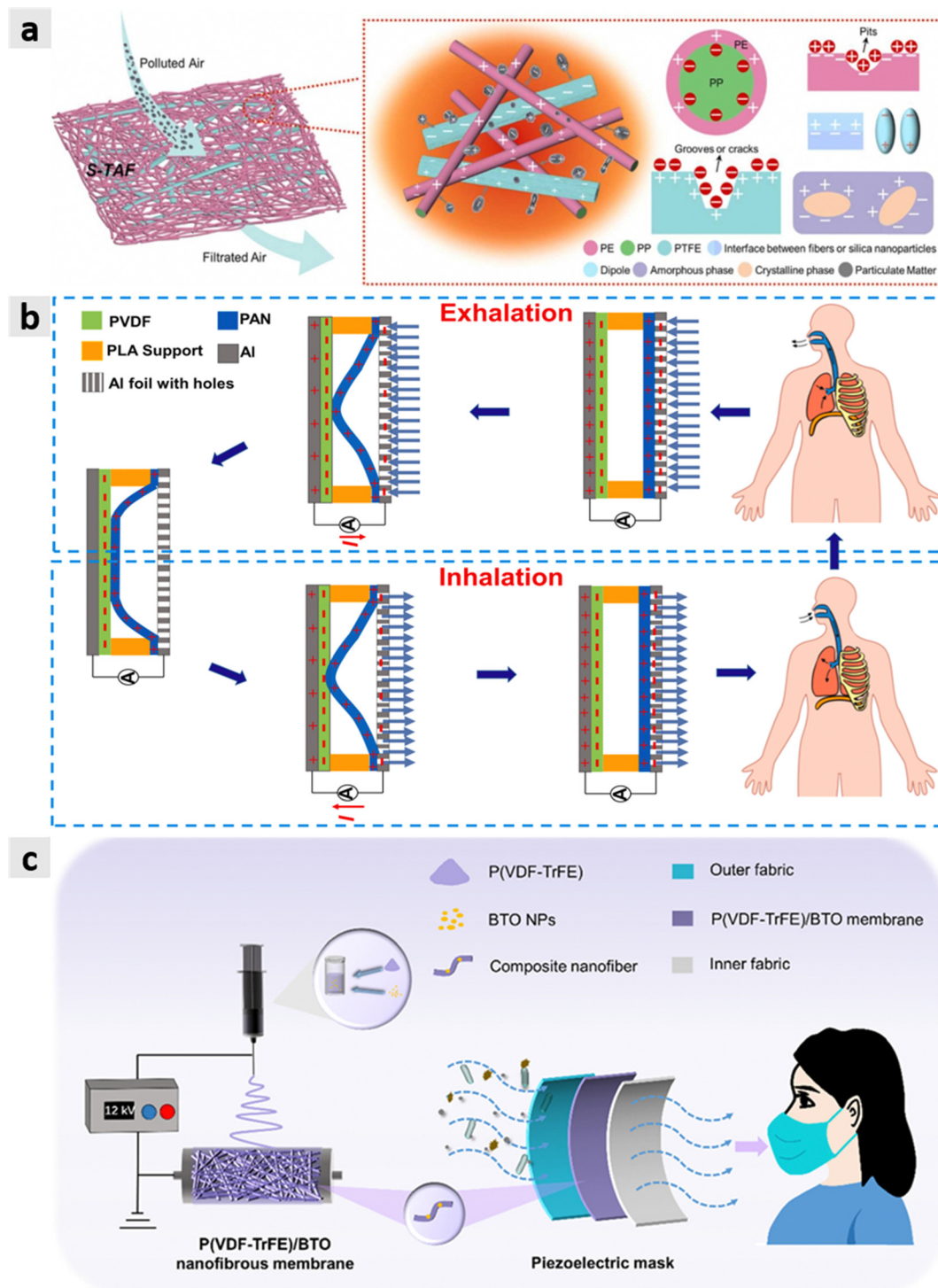
Fig. 4 (a) Schematic illustration of the filtration mechanism of S-TAF. (Reproduced with permission from ref. 27, Copyright 2023, Elsevier). (b) Schematic illustration showing how the TSF operates. (Reproduced with permission from ref. 142, Copyright 2021, Elsevier). (c) Schematic illustration of the P(VDF-TrFE)/BTO piezoelectric filter. (Reproduced with permission from ref. 145, Copyright 2023, American Chemical Society).

reported an eco-friendly self-powered filter using PLA, a material with excellent biodegradability. The two chiral structures of the lactic acid (LA) monomer, levo-LA (LLA) and dextral-LA (DLA), are polymerized into Poly-LLA (PLLA) and Poly-DLA (PDLA), which both form piezoelectricity along the polymer chain direction due to

their helical structure. After fabricating the PLLA filter through the electrospinning process, piezoelectric effects generated by airflow create electrostatic forces, allowing for additional electrical filtration. This filter exhibited a PM$_{2.5}$ removal efficiency of 99.3%, and even after 6 hours of use, it maintained a 15% improved QF.[144]

Le et al. also developed a PLLA-based piezoelectric nanofiber filter that demonstrated a low pressure drop of 91 Pa, along with a high filtration efficiency of over 99% for $PM_{2.5}$ and 91% for $PM_{1.0}$, as well as strong durability. The study highlighted that the filter could be reused after sterilization through ultrasonic cleaning, autoclaving, or microwaving and that it is an eco-friendly filter capable of fully biodegrading within 2–3 years.[29] Su et al. reported a filter with high piezoelectricity using nanofibers composed of a poly(vinylidene fluoride-trifluoroethylene) [P(VDF-TrFE)] and $BaTiO_3$ NPs (BTO NPs) mixture (Fig. 4c). The BTO NPs not only increased the dielectric constant of the filter, allowing it to store more charge but also reduced the diameter of the nanofibers and increased the surface area, thereby enhancing the mechanical filtration mechanism. This filter demonstrated a high filtration efficiency of 96% for $PM_{0.3}$ and 98% for bacteria, with a pressure drop of 182 Pa, which is about half that of commercial masks. Moreover, the filter maintained its performance after five cycles of 75% alcohol disinfection, confirming its long-term durability.[145]

3.2.3. External power source. Filtration systems powered by external sources achieve even greater filtration efficiencies compared to self-powered systems and are reported to offer additional functionalities, such as sterilization and monitoring of IAQ or health. When an electric field is formed in fiber filters through the direct supply of external electrical energy, the effect of electric filtration can be enhanced. Electrical filters are categorized into monopolar-charged filters and dipolar-induced filters.[146] The former is electrically charged and exerts strong electrostatic forces on fine pollutants for effective capture, while the latter uses an electrically induced field to capture even neutral particles. Tian and Mo designed a new electrostatic precipitator filter structure that can independently control corona charging and the polarizing field. Corona charging imparts a charge to fine particles in the air, allowing them to adhere well to the filter, while the polarizing field applies an electric field to the filter itself, helping fine particles adhere more effectively. When comparing the filtration efficiency of 0.3–0.5 μm particles using a commercial PET coarse filter, the pristine filter showed an efficiency of only 0.4%, whereas it improved to 99% when both corona charging and the polarizing field were applied. This filter enables more energy-efficient electrostatic precipitation compared to commercial filters.[147] Zhu et al. developed a filter using bio-curcumin ionic liquid (CIL) that can form a continuous electric field on the filter surface itself. This filter exhibits a filtration efficiency of 97% for $PM_{2.5}$ containing heavy metals and nano-sized viruses, thanks to its chelation effect, and maintains its performance even after long-term use of over 30 hours. Additionally, when a low voltage of 1.5 V was applied, the electrostatic field increased the particle adsorption capacity.[148] Lakshmanan et al. fabricated a transparent filter using a Nylon/chitosan-based nanofiber structure, which demonstrated a $PM_{2.5}$ removal efficiency of 95% through the strong electric field generated on the filter surface with a low voltage of 0.2 kV. This filter features an ON/OFF function to minimize energy consumption when air pollution levels are low, and thanks to the nanofiber structure containing chitosan, it is highly effective not only in removing fine PMs but also in adsorbing VOCs and suppressing viruses.[149] Professor Ko's group fabricated a transparent filter by transferring an AgNW percolation network onto a Nylon mesh (Fig. 5a). When an electric field is applied to this filter, it achieves a $PM_{2.5}$ removal efficiency of up to 99.99%, thanks to the combined effects of large-range electrostatic forces and short-range van der Waals forces. This filter also demonstrated effective antibacterial performance due to the antimicrobial properties of AgNW and was shown to be reusable after cleaning the particles adsorbed on the filter surface with polar solvents like ethylene glycol (EG). This research introduces a novel concept for air purification by combining transparency, active filtration, and reusability in a single system. The integration of advanced material science (AgNW networks) with practical design principles positions this work as a significant step forward in the development of energy-efficient, multifunctional air filters for both indoor and outdoor applications.[150] In some cases, applying an electric field can also lead to self-sterilization through Joule heating. Stanford et al. fabricated porous conductive laser-induced graphene (LIG) by performing photothermal conversion on polyimide (PI) film using a CO_2 laser cutter, and the LIG-based filter effectively captures bacteria and fine pollutants. When the filter is subjected to an electric field, it can be heated to over 300 °C through Joule heating, allowing harmful biological molecules to be decomposed and removed through high temperatures. Graphene's high thermal stability, electrical conductivity, and large surface area enable efficient trapping of PM and biological contaminants, making it highly suitable for air filtration and sterilization applications.[151] Professor Ko's group fabricated a transparent filter by transferring CuNW onto a Nylon mesh (Fig. 5b). This filter inhibits the growth of viruses through the oligodynamic effect of copper and provides a sterilization function through Joule heating, which heats the filter to over 100 °C when an electric field is applied. In addition, it achieves a $PM_{0.3}$ filtration efficiency of 93.4% due to its effective electrostatic filtration combined with the mechanical filtration mechanism. Moreover, this filter demonstrated effective reusability, with EG/ethanol cleaning removing pollutants and restoring their original properties. This study contributes significantly to the development of sustainable, multifunctional air filters, positioning itself as a solution for air quality management in healthcare, urban, and pandemic-related applications.[30] Liu et al. developed a reusable mask by fabricating an Ag micro-mesh filter. When a low voltage of 3 V was applied, the filter could rapidly heat above 60 °C in just 30 seconds through Joule heating, allowing for self-sterilization with an antibacterial efficiency of 95.58% in 20 minutes. Additionally, they demonstrated that the triboelectric effect of the PVDF membrane and polyamide 6 (PA 6) membrane enables the monitoring of breathing conditions.[152] Studies have also reported using photothermal reactions for sterilization. Xia et al. fabricated a nanofiber filter using poly(vinyl alcohol-co-ethylene), AgNPs, and PP, and this filter possesses a Janus structure with differences in wettability, giving it high moisture permeability. The AgNPs exhibited high antibacterial performance by releasing Ag^+ ions, which inhibited viral DNA replication. Additionally, through ultraviolet (UV) photothermal disinfection, the filter was heated to over 70 °C in just 120 seconds, demonstrating excellent sterilization efficiency. Moreover, by simply
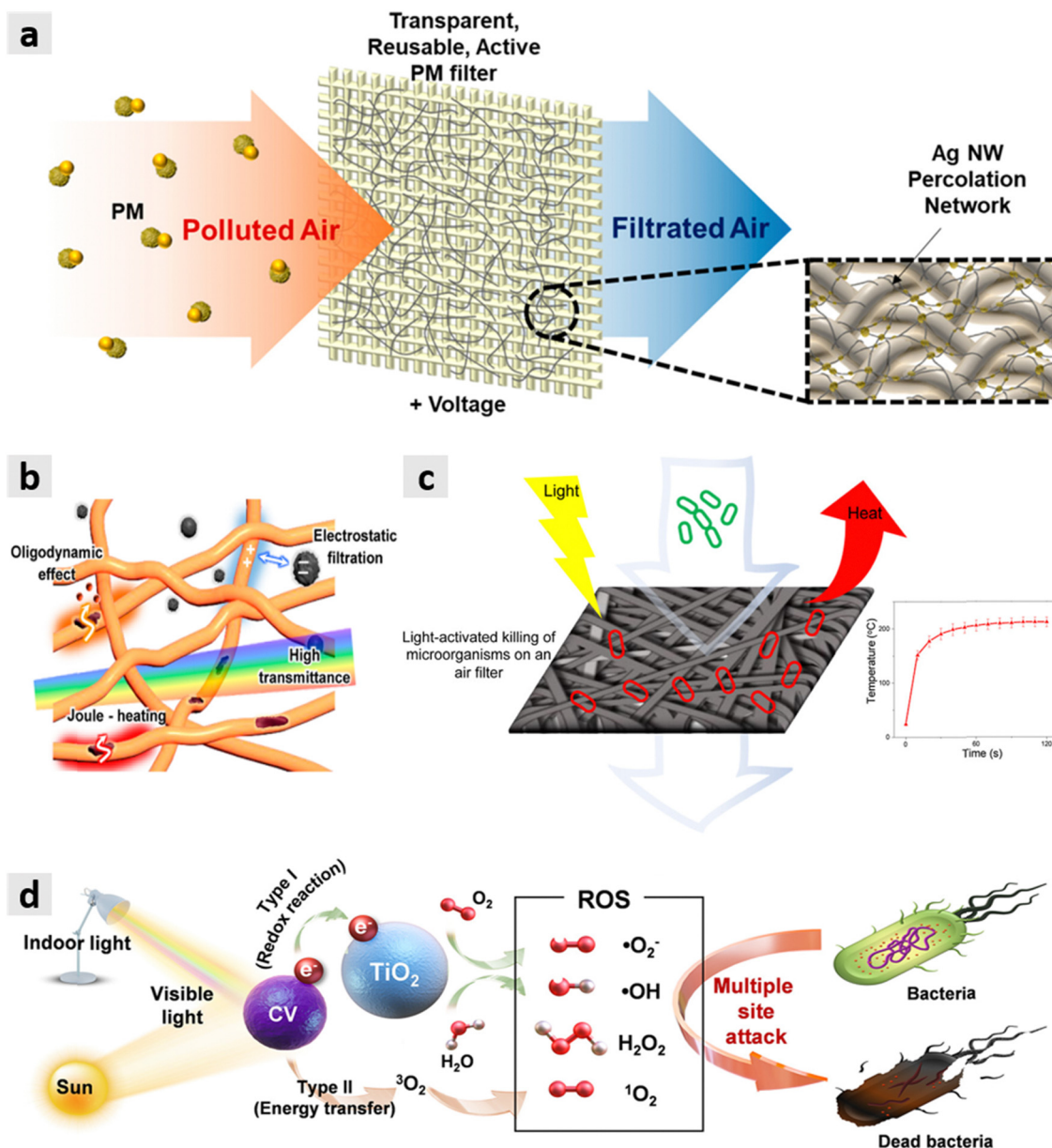
Fig. 5 (a) Schematic illustration of a transparent filter with AgNWs percolation network. (Reproduced from ref. 150, © 2017. This work is openly licensed *via* CC BY-NC 4.0). (b) Schematic illustration of a transparent filter with CuNWs and its four major capabilities. (Reproduced with permission from ref. 30, Copyright 2022, American Chemical Society). (c) Schematic illustration of photothermal sterilization. (Reproduced from ref. 154, © 2022. This work is openly licensed *via* CC-BY 4.0). (d) Schematic illustration of the mechanisms of visible-light-activated inactivation with ROS. (Reproduced with permission from ref. 155, Copyright 2021, American Chemical Society).

writing an interdigital electrode with a 6B pencil on the filter, they demonstrated that the breathing state could be monitored in real-time.[153] Demirel *et al.* fabricated a filter by incorporating halloy-site nanotubes coated with polydopamine, a photothermal agent, into e-spun PAN fibers. They demonstrated that when exposed to near-infrared (NIR) light, the filter could be rapidly heated to approximately 100 °C, effectively eliminating bacteria within 2 minutes (Fig. 5c). Additionally, the filter exhibited a bioaerosol removal efficiency of 99.97% and a QF of 0.14 Pa^{-1}.[154] Photo-catalytic reactions can also induce antibacterial effects. Heo *et al.* fabricated an antibacterial filter by spraying TiO$_2$ NPs coated with

crystal violet organic dye, which acts as a photocatalyst under visible light onto a Nylon mesh. When exposed to visible light, the photocatalytic reaction forms ROS, damaging the bacterial cell walls and DNA, resulting in an outstanding antibacterial efficiency of 99.98% (Fig. 5d). Additionally, this filter demonstrated signifi-cantly improved moisture stability by utilizing hydrophobic molecules.[155] Lee *et al.* fabricated a recyclable MOF-based photo-catalytic filter using MIL-100(Fe). This MOF has a high surface area, which allows it to effectively adsorb VOCs, and through UV photocatalytic oxidation, it generates ROS to decompose VOCs into CO$_2$ and H$_2$O, thereby removing them. The filter exhibited

94.25% adsorption efficiency and 75.95% removal efficiency of VOCs, and low-pressure drop. The unique porosity and large surface area of MOFs enable the effective adsorption and catalytic decomposition of VOCs, particularly harmful benzene, toluene, ethylbenzene, and xylene compounds, which are known to pose serious health risks even at low concentrations.[31] Studies have

also been reported on capturing pollutants effectively by generating triboelectric energy through mechanical rotation. Mo *et al.* fabricated a filter based on cellulose fiber and perfluoroethylene propylene (FEP), forming the structure of a radial piston triboelectric nanogenerator (TENG) (Fig. 6a). Mechanical rotational energy is converted into electrical energy, enabling electric
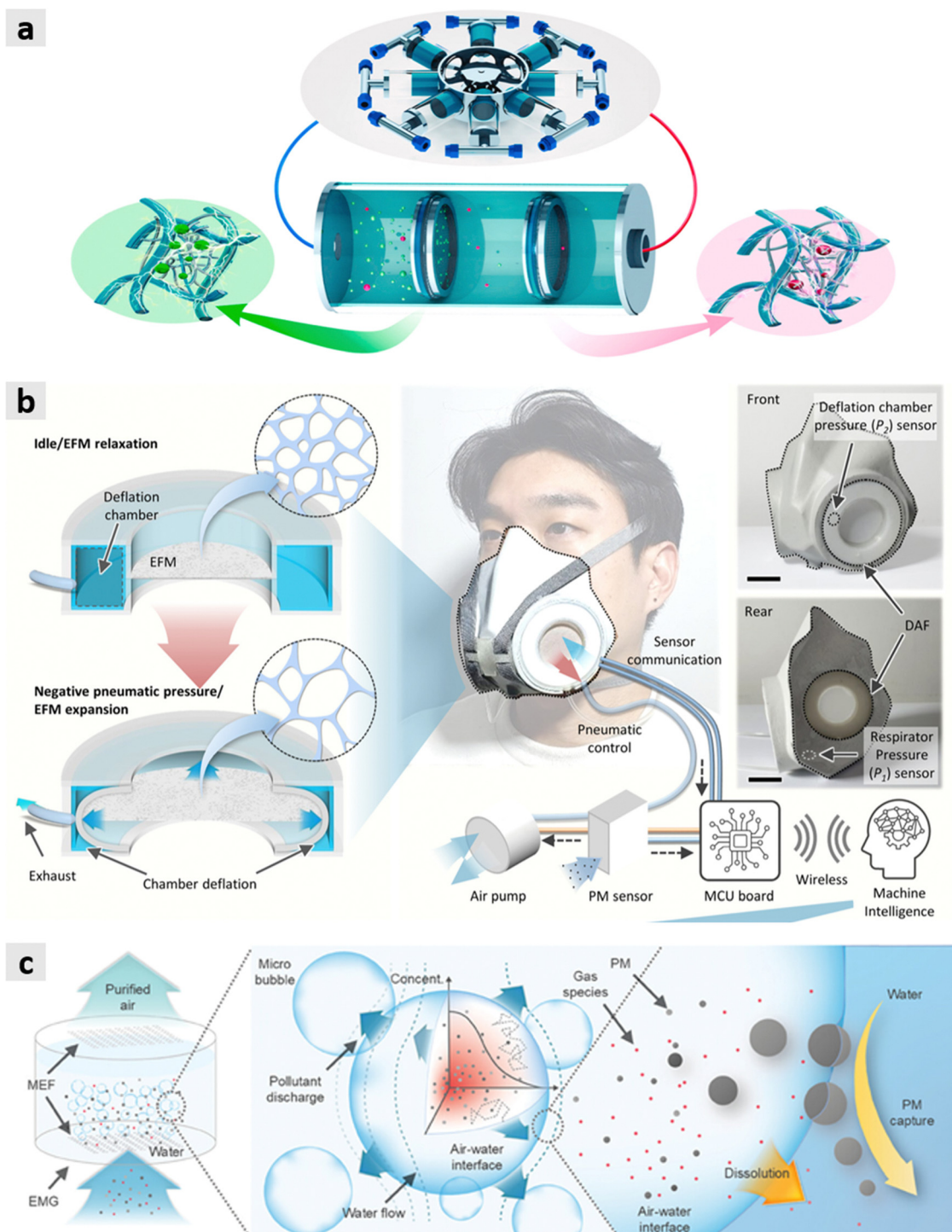

Fig. 6 (a) Schematic illustration of radial piston TENG. (Reproduced with permission from ref. 156, Copyright 2020, Elsevier). (b) A diagram and an image of a pneumatic device that mechanically deforms the filter to change the pore size. (Reproduced with permission from ref. 158, Copyright 2021, American Chemical Society). (c) Conceptual illustration of the CAPS. (Reproduced from ref. 161, © 2024. This work is openly licensed *via* CC-BY 4.0).

filtration, which, together with mechanical filtration, results in high filtration efficiency. This filter exhibited a filtration efficiency of 83.78% for $PM_{2.5}$, showing a 1.21 times higher performance compared to when it was uncharged.[156] Zheng et al. fabricated a "rotation mode high voltage TENG with direct current" (RH-DC-TENG) using high-density PE (HDPE), PTFE, and Nylon mesh. The RH-DC-TENG operates without a filter structure and removes pollutants grounded in air breakdown effects and contact electrification. In an 8000 cm^3 chamber, the RH-DC-TENG reduced $PM_{2.5}$ from 954 μg m^{-3} to 50 μg m^{-3} within 199 seconds.[157] Studies have also reported adjusting filter performance through mechanical control. Professor Ko's group developed a facial mask system that can actively adjust the filter's pore size to respond in real-time to the user's condition and surrounding environment (Fig. 6b). An e-spun stretchable poly(styrene-*b*-butadiene-*b*-styrene) (SBS) fiber membrane was used as the filter, and a pneumatic device was employed to mechanically deform the filter to adjust the pore size. Additionally, this system can automatically adjust the filter properties based on the user's breathing patterns and external air quality through a machine learning algorithm, increasing permeability or enhancing filtration efficiency when needed. This study significantly contributes to the field of respiratory protection by introducing a novel dynamic air filter (DAF) concept that combines adaptive filtration with real-time machine learning control, addressing challenges such as user discomfort, variable air quality, and energy efficiency.[158] Recently, filter technologies that analyze and customize to the user through various sensors have been reported. Professor Ko's group reported a smart mask that adjusts to various facial shapes using pressure sensors and actuators. Through a LIG-based humidity sensor and a dielectric elastomeric sponge-based pressure sensor, the mask provides real-time closed-loop feedback to monitor how well it fits the face, and it adjusts to the facial shape using two motors. Additionally, this study presented a system that stores and analyzes data, enabling real-time monitoring and alert notifications to the user through wireless Bluetooth communication. This study significantly enhances personal protective equipment by integrating adaptive fit technology and real-time monitoring using pressure and humidity sensors. By addressing the limitations of traditional masks, this research sets a foundation for next-generation smart respirators with advanced functionality and sustainability.[159] Heng et al. developed a smart mask system that collects exhaled breath inside the mask and performs multimodal analysis, allowing for continuous and non-invasive real-time health status monitoring, employing automated microfluidics, a dual cooling strategy, a wireless reading circuit, and highly selective electrochemical biosensors.[160] Additionally, studies reporting new types of filtration methods, rather than traditional filter methods, have been presented. Professor Ko's group developed a comprehensive air purification system (CAPS) that mimics the human circulatory and respiratory systems. Instead of using traditional fiber filters, they created continuous microbubbles to effectively remove CO_2, PM, and VOCs from indoor air through mass exchange driven by diffusion between liquid and gas (Fig. 6c). Pollutant removal is facilitated by the interaction between the liquid and airborne

particles. When pollutants encounter the liquid interface of the microbubbles, they are trapped and dissolved into the working liquid. This mechanism utilizes water, an eco-friendly material, with a continuous supply of clean water ensured through the circulation between external and internal microbubble generation devices. Even after operating for 5 days, the filter showed no significant changes. Therefore, it can maintain long-term performance and mimic the ability to sustain homeostasis. They fabricated the microbubble generation device with 50 μm holes by laser processing a polydimethylsiloxane (PDMS) film, enabling gas exchange between indoor and outdoor air through two generation units. CAPS reduced $PM_{2.5}$ from 1000 μg m^{-3} to below 10 μg m^{-3} within 4 minutes and lowered CO_2 concentration at a rate of -0.6% min^{-1}. This research introduces a biomimetic air purification approach, addressing critical challenges in hermetically sealed environments by integrating multifunctional capabilities such as particulate matter removal, gas exchange, and environmental sustainability. By mimicking biological processes, CAPS provides a scalable and eco-friendly solution for maintaining air quality in diverse applications, including residential, industrial, and isolated settings.[161]

4. Conclusions and outlooks

In summary, various organic (VOCs/SVOCs), inorganic, and biological air pollutants are generated indoors by building materials, cleaning products, adhesives, household items, exhaust gases, cigarette smoke, and airborne bioaerosols, which deteriorate IAQ and can cause adverse effects on humans, such as respiratory, hepatic, renal, immunological, gastrointestinal, hematological, neurological, reproductive, developmental, endocrine, dermal, and ocular issues. Prolonged exposure can even increase the risk of cancer in severe cases. To address these risks, organizations such as WHO, ASTM, ATSDR, IARC, EPA, and the Department of Health and Human Services (DHHS) have documented guidelines and established standards that regulate pollution levels based on safe exposure limits, symptoms by concentration, and exposure duration, allowing for legal enforcement of pollutant levels.

Additionally, we emphasized the need for complex filtration technologies for various substances and summarized nanotechnology-based filtration, primarily produced through electrospinning processes, as a solution. The main working principles can be broadly divided into passive filtration, self-powered filtration, and filtration operated by an external power source. In passive filtration, filter characteristics change based on fiber structure, which is influenced by the electrospinning process variables or material selection. High filter efficiency is achieved through the extensive surface area of nanofibers, and a low pressure drop is obtained due to high porosity. Many studies have been conducted on filters with excellent antibacterial properties using composite materials. In self-powered filtration, there are primarily filter technologies that use triboelectric and piezoelectric mechanisms. These filters can form their electric field, enabling electric filtration, and efficiently capture pollutants. Moreover, the generated energy allows for

the health monitoring of users. Filtration using an external power source can employ an electric filtration mechanism by applying an electric field, or perform self-sterilization through Joule heating. Sterilization can also be achieved through photothermal effects and photocatalytic reactions using light. There have been reports of effective filters that generate electrical energy through mechanical rotary devices using TENG. Additionally, systems that actively control filter performance, filters that can be monitored in real-time through various sensors, and novel air purification systems that are not fiber-based filters have also been introduced.

In addition to the substances summarized above, VOCs such as ethylene oxide (C_2H_4O), isopropyl alcohol (IPA), dimethyl sulfoxide (DMSO), and *N,N*-dimethylformamide (DMF), SVOCs like polybrominated diphenyl ethers (PBDEs) and chlorinated organophosphates, and inorganic substances such as isocyanic acid (HNCO), chlorine (Cl_2), and fluorides (F), as well as countless airborne pathogens, are generated. Research is expanding on the health effects of each of these substances. While there are fewer studies on the combined toxicity of substances compared to their independent toxicities, there are continuous reports that mixed pollutants cause more severe adverse effects. Since in real environments, multiple substances often act together, there is a pressing need for further research to improve IAQ and enhance human quality of life. Addressing this requires tackling three major challenges. First, the complexity of indoor air pollutants, which include both molecular and particulate substances, has been amplified by the increasing prevalence of bioaerosols, emphasizing the need for sterilization technologies and integrated air quality management solutions. Second, the nanomaterials used in filters can pose greater health risks to users if they widely disperse into the air or react with pollutants to form new hazardous substances. Therefore, it is essential to use biocompatible materials and nanomaterials with low reactivity. Third, the environmental impact of filter waste demands the development of innovative, eco-friendly filtration methods, such as those utilizing sustainable materials like water, to replace conventional solid-state filtration technologies. In response to these challenges, next-generation filtration technologies must leverage nanotechnology to handle the multifaceted nature of air pollutants effectively. These solutions should prioritize energy efficiency, sustainability, and minimal environmental impact, not only to enhance IAQ but also to safeguard public health and overall quality of life.

Author contributions

These authors contributed equally: Hongchan Kim, and Junhyuk Oh. Hongchan Kim: conceptualization, writing – original draft. Junhyuk Oh: conceptualization, writing – original draft. Hakbeom Lee: formal analysis, writing – review & editing. Seongmin Jeong: conceptualization, formal analysis. Seung Hwan Ko: funding acquisition, supervision, writing – review & editing.

Data availability

No primary research results, software, or code have been included and no new data were generated or analyzed as part of this review.

Conflicts of interest

There are no conflicts to declare.

Acknowledgements

References

1 F. J. Kelly and J. C. Fussell, *Environ. Geochem. Health*, 2015, **37**, 631–649.
2 W. P. Logan, *Lancet*, 1953, **261**, 336–338.
3 J. B. Sanderson, *Political Stud.*, 1961, **9**, 236–253.
4 C. D. Ahlers, *Envtl. l*, 2015, **45**, 75.
5 H. Yue, C. He, Q. Huang, D. Yin and B. A. Bryan, *Nat. Commun.*, 2020, **11**, 1462.
6 B. P. Singh, *MRS Energy Sustainability*, 2024, 1–26.
7 A. J. Chauhan and S. L. Johnston, *Br. Med. Bull.*, 2003, **68**, 95–112.
8 A. Nel, *Science*, 2005, **308**, 804–806.
9 K. Ahn, *J. Allergy Clin. Immunol.*, 2014, **134**, 993–999.
10 H. Kim, W.-H. Kim, Y.-Y. Kim and H.-Y. Park, *Front. Public Health*, 2020, **8**, 575330.
11 J. Wiley, J. Robinson, T. Piazza, K. Garrett, K. Cirksena, Y. Cheng and G. Martin, *Survey Research Centre*, University of California, Berkeley. California Air Resources Board NL-w AK, 1991, 17722.
12 A. P. Jones, *Atmos. Environ.*, 1999, **33**, 4535–4564.
13 Z. Noorimotlagh, N. Jaafarzadeh, S. S. Martínez and S. A. Mirzaee, *Environ. Res.*, 2021, **193**, 110612.
14 S. E. Gillooly, Y. Zhou, J. Vallarino, M. T. Chu, D. R. Michanowicz, J. I. Levy and G. Adamkiewicz, *Environ. Pollut.*, 2019, **244**, 440–450.
15 T. H. Nasution, A. Hizriadi, K. Tanjung and F. Nurmayadi, presented in part at 2020 4th International Conference on Electrical, Telecommunication and Computer Engineering (ELTICOM), Medan, September, 2020.
16 S. Bhattacharya, S. Sridevi and R. Pitchiah, presented in part at 2012 Sixth International Conference on Sensing Technology (ICST), Kolkata, December, 2012.
17 T. Godish and J. D. Spengler, *Indoor Air*, 1996, **6**, 135–145.
18 J. M. Daisey, W. J. Angell and M. G. Apte, *Indoor Air*, 2003, **13**, 53–64.
19 G. Liu, M. Xiao, X. Zhang, C. Gal, X. Chen, L. Liu, S. Pan, J. Wu, L. Tang and D. Clements-Croome, *Sustain. Cities Soc.*, 2017, **32**, 375–396.
20 A. Luengas, A. Barona, C. Hort, G. Gallastegui, V. Platel and A. Elias, *Rev. Environ. Sci. Biotechnol.*, 2015, **14**, 499–522.
21 W. C. Hinds and Y. Zhu, *Aerosol technology: properties, behavior, and measurement of airborne particles*, John Wiley & Sons, 2022.
22 R. Brown, *J. Aerosol Sci.*, 1981, **12**, 349–356.
23 Z. Sun, Y. Kong, L. Lan, Y. Meng, T. You, R. Pauer, H. Wang, Y. Zhang, M. Tang and A. Demello, *Small*, 2024, 2301074.
24 H. Souzandeh, K. S. Johnson, Y. Wang, K. Bhamidipaty and W.-H. Zhong, *ACS Appl. Mater. Interfaces*, 2016, **8**, 20023–20031.
25 Z. Wang, C. Zhao and Z. Pan, *J. Colloid Interface Sci.*, 2015, **441**, 121–129.
26 J. H. Jung, G. B. Hwang, J. E. Lee and G. N. Bae, *Langmuir*, 2011, **27**, 10256–10264.
27 Y. Wang, X. Zhang, X. Jin and W. Liu, *Nano Energy*, 2023, **105**, 108021.

28 L. Wang, Y. Bian, C. K. Lim, Z. Niu, P. K. Lee, C. Chen, L. Zhang, W. A. Daoud and Y. Zi, *Nano Energy*, 2021, **85**, 106015.

29 T. T. Le, E. J. Curry, T. Vinikoor, R. Das, Y. Liu, D. Sheets, K. T. Tran, C. J. Hawxhurst, J. F. Stevens and J. N. Hancock, *Adv. Funct. Mater.*, 2022, **32**, 2113040.

30 S. Han, J. Kim, Y. Lee, J. Bang, C. G. Kim, J. Choi, J. Min, I. Ha, Y. Yoon and C.-H. Yun, *Nano Lett.*, 2021, **22**, 524–532.

31 J. Lee, J. Jang, J. Kim and S.-H. Lim, *Chem. Eng. J.*, 2022, **430**, 132891.

32 S. United States. Agency for Toxic, R. Disease and C. Syracuse Research, *Toxicological profile for benzene*, U.S. Dept. of Health and Human Services, Public Health Service, Agency for Toxic Substances and Disease Registry, Atlanta, Ga, 2007.

33 J. Taylor, S. United States. Agency for Toxic and R. Disease, *Toxicological profile for ethylbenzene*, U.S. Dept. of Health and Human Services, Public Health Service, Agency for Toxic Substances and Disease Registry, Atlanta, Ga, 2010.

34 S. United States. Agency for Toxic and R. Disease, *Toxicological profile for xylene*, U.S. Dept. of Health and Human Services, Public Health Service, Agency for Toxic Substances and Disease Registry, Atlanta, Ga, 2007.

35 S. United States. Agency for Toxic and R. Disease, *Toxicological profile for styrene*, U.S. Dept. of Health and Human Services, Public Health Service, Agency for Toxic Substances and Disease Registry, Atlanta, Ga, 2010.

36 A. Dorsey, S. United States. Agency for Toxic, R. Disease, H. United States. Department of and S. Human, *Toxicological profile for toluene*, Agency for Toxic Substances and Disease Registry, Atlanta, Ga, 2000.

37 H. El-Masri, S. United States. Agency for Toxic, R. Disease, A. United States. Environmental Protection and C. Syracuse Research, *Toxicological profile for naphthalene, 1-methylnaphthalene, and 2-methylnaphthalene*, U.S. Dept. of Health and Human Services, Public Health Service, Agency for Toxic Substances and Disease Registry, Atlanta, Ga, 2005.

38 S. United States. Agency for Toxic and R. Disease, *Toxicological profile for formaldehyde*, U.S. Dept. of Health & Human Services, Public Health Service, Agency for Toxic Substances and Disease Registry, Atlanta, Ga, 1999.

39 S. United States. Agency for Toxic and R. Disease, *Toxicological profile for trichloroethylene*, U.S. Department of Health and Human Services, Agency for Toxic Substances and Disease Registry, Atlanta, Georgia, June 2019 edition, 2019.

40 S. United States. Agency for Toxic and R. Disease, *Toxicological profile for tetrachloroethylene*, U.S. Department of Health & Human Services, Agency for Toxic Substances and Disease Registry, Atlanta, Georgia, June 2019 edition, 2019.

41 S. United States. Agency for Toxic and R. Disease, *Toxicological profile for 1,3-butadiene*, U.S. Department of Health and Human Services, Public Health Service, Agency for Toxic Substances and Disease Registry, Atlanta, Georgia, 2012.

42 C. Syracuse Research, C. Clement International, S. United States. Agency for Toxic and R. Disease, *Toxicological profile for chloroform*, U.S. Dept. of Health and Human Services, Public Health Service, Agency for Toxic Substances and Disease Registry, Atlanta, Ga, 1993.

43 S. United States. Agency for Toxic and R. Disease, *Toxicological profile for 2-butanone*, U.S. Department of Health and Human Services, Agency for Toxic Substances and Disease Registry, Atlanta, Ga, October 2020 edition, 2020.

44 N. Roney, S. United States. Agency for Toxic and R. Disease, *Toxicological profile for acrolein*, U.S. Departtment of Health and Human Services, Public Health Service, Agency for Toxic Substances and Disease Registry, Atlanta, Georgia, Update. edn., 2007.

45 S. United States. Agency for Toxic and R. Disease, *Toxicological profile for acetone*, U.S. Dept. of Health and Human Services, Public Health Service, Agency for Toxic Substances and Disease Registry, Atlanta, Ga, 1994.

46 S. United States. Agency for Toxic and R. Disease, *Toxicological profile for DDT, DDE, and DDD*, U.S. Department of Health and Human Services, Agency for Toxic Substances and Disease Registry, Atlanta, Ga, April 2022 edition, 2022.

47 S. United States. Agency for Toxic, R. Disease and C. Syracuse Research, *Toxicological profile for heptachlor and heptachlor epoxide*, U.S. Dept. of Health and Human Services, Public Health Service, Agency for Toxic Substances and Disease Registry, Atlanta, Ga, 2007.

48 S. United States. Agency for Toxic and R. Disease, *Toxicological profile for chlordane*, U.S. Department of Health and Human Services, Agency for Toxic Substances and Disease Registry, Atlanta, Ga., February 2018 edition, 2018.

49 S. United States. Agency for Toxic and R. Disease, *Toxicological profile for polychlorinated biphenyls (PCBs)*, U.S. Dept. of Health and Human Services, Public Health Service, Agency for Toxic Substances and Disease Registry, Atlanta, GA, 2000.

50 S. United States. Agency for Toxic, R. Disease and I. Research Triangle, *Toxicological profile for polycyclic aromatic hydrocarbons*, U.S. Dept. of Health and Human Services, Public Health Service, Agency for Toxic Substances and Disease Registry, Atlanta, Ga, 1995.

51 S. United States. Agency for Toxic and R. Disease, *Toxicological profile for di(2-ethylhexyl)phthalate (DEHP): draft for public comment*, U.S. Department of Health and Human Services, Agency for Toxic Substances and Disease Registry, Atlanta, Ga, December 2019 edition, 2019.

52 T. A. Jacobson, J. S. Kler, M. T. Hernke, R. K. Braun, K. C. Meyer and W. E. Funk, *Nat. Sustainability*, 2019, **2**, 691–701.

53 K. E. Schaefer, *Experientia*, 1982, **38**, 1163–1168.

54 D. Robertson, *Med. Hypotheses*, 2001, **56**, 513–518.

55 J. R. Goldsmith and S. A. Landaw, *Science*, 1968, **162**, 1352–1359.

56 F. Villanueva, M. Ródenas, A. Ruus, J. Saffell and M. F. Gabriel, *Appl. Spectrosc. Rev.*, 2022, **57**, 531–579.

57 U. EPA, US Environmental Protection Agency, Washington, DC, 2016.

58 World Health Organization, *WHO global air quality guidelines: particulate matter (PM2.5 and PM10), ozone, nitrogen dioxide, sulfur dioxide and carbon monoxide*, World Health Organization, Geneva, 1st edn, 2021.

59 M. Amann, *Health risks of ozone from long-range transboundary air pollution*, WHO Regional Office Europe, 2008.

60 D. Nuvolone, D. Petri and F. Voller, *Environ. Sci. Pollut. Res.*, 2018, **25**, 8074–8088.

61 J. Pravda, *Mol. Med.*, 2020, **26**, 41.

62 World Health Organization, *Air quality guidelines for Europe*, World Health Organization, Regional Office for Europe, 2000.

63 Z. Chen, N. Liu, H. Tang, X. Gao, Y. Zhang, H. Kan, F. Deng, B. Zhao, X. Zeng and Y. Sun, *Indoor Air*, 2022, **32**, e13170.

64 S. Feng, D. Gao, F. Liao, F. Zhou and X. Wang, *Ecotoxicol. Environ. Saf.*, 2016, **128**, 67–74.

65 E. Terzi, G. Argyropoulos, A. Bougatioti, N. Mihalopoulos, K. Nikolaou and C. Samara, *Atmos. Environ.*, 2010, **44**, 2231–2239.

66 S. United States. Agency for Toxic and R. Disease, *Toxicological profile for ammonia*, U.S. Dept. of Health and Human Services, Public Health Service, Agency for Toxic Substances and Disease Registry, Atlanta, Ga, 2004.

67 D. J. Jarvis, G. Adamkiewicz, M. E. Heroux, R. Rapp and F. J. Kelly, *WHO guidelines for indoor air quality: selected pollutants*, World Health Organization, Regional Office for Europe, Copenhagen, Denmark, 2010.

68 L. Song, J. Zhou, C. Wang, G. Meng, Y. Li, M. Jarin, Z. Wu and X. Xie, *J. Hazard. Mater.*, 2022, **424**, 127429.

69 C. Gonzalez-Martin, *Encycl. Microbiol.*, 2019, 52.

70 H. Myung and Y. S. Joung, *Environ. Sci. Technol.*, 2024, **58**, 6846–6867.

71 J. D. Spengler and K. Sexton, *Science*, 1983, **221**, 9–17.

72 S. Nandasena, A. Wickremasinghe and N. Sathiakumar, *Indoor Environmental Quality and Health Risk toward Healthier Environment for All*, 2020, pp. 237–250.

73 X. Tang, P. K. Misztal, W. W. Nazaroff and A. H. Goldstein, *Environ. Sci. Technol.*, 2016, **50**, 12686–12694.

74 J. D. Fenske and S. E. Paulson, *J. Air Waste Manage. Assoc.*, 1999, **49**, 594–598.

75 E. G. Elliott, P. Trinh, X. Ma, B. P. Leaderer, M. H. Ward and N. C. Deziel, *Sci. Total Environ.*, 2017, **576**, 138–147.

76 S. H. Lamm, A. Engel, K. P. Joshi, D. M. Byrd III and R. Chen, *Chem.-Biol. Interact.*, 2009, **182**, 93–97.

77 J. Y. Chin, C. Godwin, E. Parker, T. Robins, T. Lewis, P. Harbin and S. Batterman, *Indoor Air*, 2014, **24**, 403–415.

78 J. Wang, C. Janson, T. Gislason, M. Gunnbjörnsdottir, R. Jogi, H. Orru and D. Norbäck, *Environ. Pollut.*, 2023, **321**, 121103.

79 C. Freire, R. Ramos, R. Puertas, M.-J. Lopez-Espinosa, J. Julvez, I. Aguilera, F. Cruz, M.-F. Fernandez, J. Sunyer and N. Olea, *Br. J. Prev. Soc. Med.*, 2010, **64**, 223–228.

80 A. Mazzatenta, M. Pokorski, F. Sartucci, L. Domenici and C. Di Giulio, *Respir. Physiol. Neurobiol.*, 2015, **209**, 81–84.

81 R. American Society of Heating, C. Air-Conditioning Engineers and I. American National Standards, *Ventilation and acceptable indoor air quality*, American Society of Heating, Refrigerating and Air-Conditioning Engineers, Atlanta, GA, 2022.

82 Z. Peng and J. L. Jimenez, *Environ. Sci. Technol. Lett.*, 2021, **8**, 392–397.

83 U. EU, *Off. J. Eur. Union*, 2016, **50**, 334.

84 P. Wolkoff, *Int. J. Hyg. Environ. Health*, 2020, **225**, 113439.

85 F. Dominici, Y. Wang, A. W. Correia, M. Ezzati, C. A. Pope III and D. W. Dockery, *Epidemiology*, 2015, **26**, 556–564.

86 M. Li, C. J. Weschler, G. Beko, P. Wargocki, G. Lucic and J. Williams, *Environ. Sci. Technol.*, 2020, **54**, 5419–5428.

87 S. United States. Occupational, A. Health and A. United States. Environmental Protection, *OSHA occupational chemical database*, U.S. Dept. of Labor, Occupational Safety & Health Administration, Washington, DC.

88 H.-A. H. Dang and C. V. Nguyen, *World Dev.*, 2021, **140**, 105296.

89 M. Lenzen, M. Li, A. Malik, F. Pomponi, Y.-Y. Sun, T. Wiedmann, F. Faturay, J. Fry, B. Gallego and A. Geschke, *PLoS One*, 2020, **15**, e0235654.

90 R. L. Riley, C. Mills, F. O'grady, L. Sultan, F. Wittstadt and D. Shivpuri, *Am. Rev. Respir. Dis.*, 1962, **85**, 511–525.

91 R. Riley, *Environ. Int.*, 1982, **8**, 317–320.

92 F. M. Blachere, W. G. Lindsley, T. A. Pearce, S. E. Anderson, M. Fisher, R. Khakoo, B. J. Meade, O. Lander, S. Davis and R. E. Thewlis, *Clin. Infect. Dis.*, 2009, **48**, 438–440.

93 P. Srikanth, S. Sudharsanam and R. Steinberg, *Indian J. Med. Microbiol.*, 2008, **26**, 302–312.

94 P. Kumar, M. A. Kausar, A. Singh and R. Singh, *Air Qual., Atmos. Health*, 2021, **14**, 1723–1736.

95 A. Fernstrom and M. Goldblatt, *J. Pathog.*, 2013, 493960.

96 V. Neira, P. Rabinowitz, A. Rendahl, B. Paccha, S. G. Gibbs and M. Torremorell, *PLoS One*, 2016, **11**, e0146616.

97 M. O. Fernandez, R. J. Thomas, N. J. Garton, A. Hudson, A. Haddrell and J. P. Reid, *J. R. Soc., Interface*, 2019, **16**, 20180779.

98 L. Martinez, R. Verma, J. Croda, C. R. Horsburgh, K. S. Walter, N. Degner, K. Middelkoop, A. Koch, S. Hermans and D. F. Warner, *Eur. Respir. J.*, 2019, 53.

99 J. Duguid, *Epidemiol. Infect.*, 1946, **44**, 471–479.

100 K. H. Bartlett, S. M. Kennedy, M. Brauer, C. van Netten and B. Dill, *J. Occup. Environ. Hyg.*, 2004, **1**, 639–647.

101 W. W. F. Leung and Q. Sun, *Sep. Purif. Technol.*, 2020, **250**, 116886.

102 C. Burger, B. S. Hsiao and B. Chu, *Annu. Rev. Mater. Res.*, 2006, **36**, 333–368.

103 F. Karabulut, *Environ. Sci.*, 2020, 222450950.

104 M. Wang, B. Yu, J. Han, W. Song and F. Zhu, *J. Ind. Text.*, 2017, **46**, 1281–1293.

105 S. Y. Kim, P. Purnama and S. H. Kim, *Macromol. Res.*, 2010, **18**, 1233–1236.

106 L. Xia, P. Xi and B. Cheng, *Mater. Lett.*, 2015, **147**, 79–81.

107 J. Xue, T. Wu, Y. Dai and Y. Xia, *Chem. Rev.*, 2019, **119**, 5298–5415.

108 T. Lu, J. Cui, Q. Qu, Y. Wang, J. Zhang, R. Xiong, W. Ma and C. Huang, *ACS Appl. Mater. Interfaces*, 2021, **13**, 23293–23313.

109 J. Choi, B. J. Yang, G.-N. Bae and J. H. Jung, *ACS Appl. Mater. Interfaces*, 2015, **7**, 25313–25320.

110 D. Cho, A. Naydich, M. W. Frey and Y. L. Joo, *Polymer*, 2013, **54**, 2364–2372.

111 R. Hao, S. Yang, K. Yang, Z. Zhang, T. Wang, S. Sang and H. Zhang, *ACS Appl. Energy Mater.*, 2021, **4**, 14700–14708.

112 Z. Peng, J. Shi, X. Xiao, Y. Hong, X. Li, W. Zhang, Y. Cheng, Z. Wang, W. J. Li and J. Chen, *Nat. Commun.*, 2022, **13**, 7835.

113 Y. Cheng, C. Wang, J. Zhong, S. Lin, Y. Xiao, Q. Zhong, H. Jiang, N. Wu, W. Li and S. Chen, *Nano Energy*, 2017, **34**, 562–569.

114 D. H. Reneker and A. L. Yarin, *Polymer*, 2008, **49**, 2387–2425.

115 J. Xue, J. Xie, W. Liu and Y. Xia, *Acc. Chem. Res.*, 2017, **50**, 1976–1987.

116 J. Xie, X. Li and Y. Xia, *Macromol. Rapid Commun.*, 2008, **29**, 1775–1792.

117 W. Nuansing, E. Georgilis, T. V. de Oliveira, G. Charalambidis, A. Eleta, A. G. Coutsolelos, A. Mitraki and A. M. Bittner, *Part. Part. Syst. Charact.*, 2014, **31**, 88–93.

118 L. Jørgensen, K. Qvortrup and I. S. Chronakis, *RSC Adv.*, 2015, **5**, 53644–53652.

119 J.-F. Xu, Y.-Z. Chen, D. Wu, L.-Z. Wu, C.-H. Tung and Q.-Z. Yang, *Angew. Chem., Int. Ed.*, 2013, **52**, 9738–9742.

120 J. Jang, B. G. Hyun, S. Ji, E. Cho, B. W. An, W. H. Cheong and J.-U. Park, *NPG Asia Mater.*, 2017, **9**, e432.

121 J. Geltmeyer, J. De Roo, F. Van den Broeck, J. C. Martins, K. De Buysser and K. De Clerck, *J. Sol-Gel Sci. Technol.*, 2016, **77**, 453–462.

122 J. E. Efome, D. Rana, T. Matsuura and C. Q. Lan, *J. Mater. Chem. A*, 2018, **6**, 4550–4555.

123 D. Malwal and P. Gopinath, *Environ. Sci.: Nano*, 2015, **2**, 78–85.

124 C. D. Saquing, C. Tang, B. Monian, C. A. Bonino, J. L. Manasco, E. Alsberg and S. A. Khan, *Ind. Eng. Chem. Res.*, 2013, **52**, 8692–8704.

125 Y. Zheng, H. Cao, Z. Zhou, X. Mei, L. Yu, X. Chen, G. He, Y. Zhao, D. Wu and D. Sun, *Fibers Polym.*, 2019, **20**, 1180–1186.

126 A. Yarin, *Polym. Adv. Technol.*, 2011, **22**, 310–317.

127 K. Liu, C. Liu, P.-C. Hsu, J. Xu, B. Kong, T. Wu, R. Zhang, G. Zhou, W. Huang and J. Sun, *ACS Cent. Sci.*, 2018, **4**, 894–898.

128 J. Matulevicius, L. Kliucininkas, D. Martuzevicius, E. Krugly, M. Tichonovas and J. Baltrusaitis, *J. Nanomater.*, 2014, 859656.

129 S. Zhang, H. Liu, N. Tang, N. Ali, J. Yu and B. Ding, *ACS Nano*, 2019, **13**, 13501–13512.

130 X. Li, C. Wang, X. Huang, T. Zhang, X. Wang, M. Min, L. Wang, H. Huang and B. S. Hsiao, *ACS Appl. Mater. Interfaces*, 2018, **10**, 42891–42904.

131 C. Liu, P.-C. Hsu, H.-W. Lee, M. Ye, G. Zheng, N. Liu, W. Li and Y. Cui, *Nat. Commun.*, 2015, **6**, 6205.

132 S. Mallakpour, E. Azadi and C. M. Hussain, *Adv. Colloid Interface Sci.*, 2022, **303**, 102653.

133 M. Oproescu, O. Ahmed, G.-V. Iana, M. M. Dicu, A. M. Balteanu and M. Baldea, presented in part at 2023 15th International Conference on Electronics, Computers and Artificial Intelligence (ECAI), Bucharest, June, 2023.

134 V. Liapun and M. Motola, *Handbook of Functionalized Carbon Nanostructures: From Synthesis Methods to Applications*, 2023, pp. 1–38.

135 Y.-S. Ko, Y. H. Joe, M. Seo, K. Lim, J. Hwang and K. Woo, *J. Mater. Chem. B*, 2014, **2**, 6714–6722.

136 H. Souzandeh, B. Molki, M. Zheng, H. Beyenal, L. Scudiero, Y. Wang and W.-H. Zhong, *ACS Appl. Mater. Interfaces*, 2017, **9**, 22846–22855.

137 W. Jung, J. S. Lee, S. Han, S. H. Ko, T. Kim and Y. H. Kim, *J. Mater. Chem. A*, 2018, **6**, 16975–16982.

138 Y. Zhao, Z. Zhong, Z.-X. Low and Z. Yao, *RSC Adv.*, 2015, **5**, 91951–91959.

139 Z. L. Wang and A. C. Wang, *Mater. Today*, 2019, **30**, 34–51.

140 Y. Bai, C. B. Han, C. He, G. Q. Gu, J. H. Nie, J. J. Shao, T. X. Xiao, C. R. Deng and Z. L. Wang, *Adv. Funct. Mater.*, 2018, **28**, 1706680.

141 Y. Hu, Y. Wang, S. Tian, A. Yu, L. Wan and J. Zhai, *Macromol. Mater. Eng.*, 2021, **306**, 2100128.

142 H. He, J. Guo, B. Illés, A. Géczy, B. Istók, V. Hliva, D. Török, J. G. Kovács, I. Harmati and K. Molnár, *Nano Energy*, 2021, **89**, 106418.

143 M. T. Chorsi, E. J. Curry, H. T. Chorsi, R. Das, J. Baroody, P. K. Purohit, H. Ilies and T. D. Nguyen, *Adv. Mater.*, 2019, **31**, 1802084.

144 J. Zhang, S. Gong, C. Wang, D. Y. Jeong, Z. L. Wang and K. Ren, *Macromol. Mater. Eng.*, 2019, **304**, 1900259.

145 C. Su, L. Zhang, Y. Zhang, X. Huang, Y. Ye, Y. Xia, Z. Gong, X. Qin, Y. Liu and S. Guo, *ACS Appl. Mater. Interfaces*, 2023, **15**, 5845–5855.

146 C. Gao, E. Tian, Y. Zhang and J. Mo, *Appl. Mater. Today*, 2022, **26**, 101369.

147 E. Tian and J. Mo, *Energy Build.*, 2019, **186**, 276–283.

148 Q.-H. Zhu, G.-H. Zhang, L. Zhang, J. Fu, Y.-R. Zhou, Y.-Q. Xiang, L. Ma, G.-H. Tao and L. He, *Chem. Eng. J.*, 2022, **449**, 137788.

149 A. Lakshmanan, G. Marappan and D. Sarkar, *Chem. Eng. J.*, 2023, **461**, 142023.

150 S. Jeong, H. Cho, S. Han, P. Won, H. Lee, S. Hong, J. Yeo, J. Kwon and S. H. Ko, *Nano Lett.*, 2017, **17**, 4339–4346.

151 M. G. Stanford, J. T. Li, Y. Chen, E. A. McHugh, A. Liopo, H. Xiao and J. M. Tour, *ACS Nano*, 2019, **13**, 11912–11920.

152 W. Liu, Y. Sun, A. Cui, Y. Xia, Q. Yan, Y. Song, L. Wang, G. Shan and X. Wang, *Nano Energy*, 2023, **105**, 107987.

153 M. Xia, Z. Yao, Z. Xiong, Y. Wu, P. Cheng, Q. Cheng, J. Xu, X. Wang, K. Liu and D. Wang, *Adv. Mater. Interfaces*, 2023, **10**, 2201952.

154 O. Demirel, S. Kolgesiz, S. Yuce, S. Hayat Soytaş, D. Y. Koseoglu-Imer and H. Unal, *ACS Appl. Nano Mater.*, 2022, **5**, 18127–18137.

155 K. J. Heo, S. B. Jeong, J. Shin, G. B. Hwang, H. S. Ko, Y. Kim, D. Y. Choi and J. H. Jung, *Nano Lett.*, 2020, **21**, 1576–1583.

156 J. Mo, C. Zhang, Y. Lu, Y. Liu, N. Zhang, S. Wang and S. Nie, *Nano Energy*, 2020, **78**, 105357.

157 Q. Zheng, L. Fang, X. Tang, L. Zheng and H. Li, *Nano Energy*, 2022, **97**, 107183.

158 J. Shin, S. Jeong, J. Kim, Y. Y. Choi, J. Choi, J. G. Lee, S. Kim, M. Kim, Y. Rho and S. Hong, *ACS Nano*, 2021, **15**, 15730–15740.

159 K. Kwon, Y. J. Lee, Y. Jung, I. Soltis, Y. Na, L. Romero, M. C. Kim, N. Rodeheaver, H. Kim and C. Lee, *Biomaterials*, 2024, 122866.

160 W. Heng, S. Yin, J. Min, C. Wang, H. Han, E. Shirzaei Sani, J. Li, Y. Song, H. B. Rossiter and W. Gao, *Science*, 2024, **385**, 954–961.

161 S. Jeong, J. Shin, J. Kim, H. Kim, J. G. Lee, J. Min, S. Hong and S. H. Ko, *Adv. Mater.*, 2024, **36**, 2405568.